

Department of Signal Processing and Acoustics

# Analyzing Performance of Mobile MIMO-OFDM Wireless Systems: Tools and Results

---

Alexandra Oborina





# Analyzing Performance of Mobile MIMO-OFDM Wireless Systems: Tools and Results

**Alexandra Oborina**

A doctoral dissertation completed for the degree of Doctor of Science in Technology to be defended, with the permission of the Aalto University School of Electrical Engineering, at a public examination held at the lecture hall S1 of the school on 21st of September 2012 at 12 noon.

**Aalto University**  
**School of Electrical Engineering**  
**Department of Signal Processing and Acoustics**

**Supervising professor**

Academy Prof. Visa Koivunen

**Thesis advisor**

Academy Prof. Visa Koivunen

**Preliminary examiners**

Prof. Tapani Ristaniemi, University of Jyväskylä, Finland

Dr. Samuli Visuri, Nokia, Finland

**Opponents**

Prof. Tapani Ristaniemi, University of Jyväskylä, Finland

Assoc. Prof. Kimmo Kansanen, NTNU, Norway

Aalto University publication series

**DOCTORAL DISSERTATIONS** 110/2012

© Alexandra Oborina

ISBN 978-952-60-4753-9 (printed)

ISBN 978-952-60-4754-6 (pdf)

ISSN-L 1799-4934

ISSN 1799-4934 (printed)

ISSN 1799-4942 (pdf)

<http://urn.fi/URN:ISBN:978-952-60-4754-6>

Unigrafia Oy

Helsinki 2012

Finland



**Author**

Alexandra Oborina

**Name of the doctoral dissertation**

Analyzing Performance of Mobile MIMO-OFDM Wireless Systems: Tools and Results

**Publisher** School of Electrical Engineering**Unit** Department of Signal Processing and Acoustics**Series** Aalto University publication series DOCTORAL DISSERTATIONS 110/2012**Field of research** Signal Processing**Manuscript submitted** 21 August 2012**Date of the defence** 21 September 2012**Permission to publish granted (date)** 21 August 2012**Language** English **Monograph** **Article dissertation (summary + original articles)****Abstract**

Multi-antenna and multi-carrier wireless transmission techniques are expected to provide high peak data rates and spectral efficiency, good coverage and reliable transmission required by emerging wireless standards such as 3GPP Long Term Evolution (LTE) and 3GPP LTE-Advanced. The multi-stream transmission via Multiple-Output Multiple-Input (MIMO) systems achieves different gains using beamforming, spatial diversity and spatial multiplexing techniques. The multi-carrier modulation via Orthogonal Frequency Division Multiplexing (OFDM) enhances spectral efficiency and facilitates using simple transceiver structures for broadband communications.

MIMO-OFDM transmission impacts the design of many physical-level, system-level and radio resource management (RRM) functions as well as interaction between link and system level called Link-to-System (L2S) interface. In this thesis methods for optimizing L2S interface and RRM for MIMO-OFDM wireless systems and performance measures suitable for the system level performance evaluation are developed. The derived techniques are needed in network planning and optimization in order to analyze coverage, interference, frequency utilization, traffic loading. Moreover, they are used in dynamic system level simulations.

In this thesis a computational efficient method for calculating the effective Signal-to-Interference-and-Noise-Ratio (SINR) mapping as advanced L2S interface for MIMO-OFDM transmission at the system-level is introduced. Asymptotic distribution of the effective SINR is established. In case of fast link adaptation with adaptive modulation and coding a mixture distribution model is used. The established distribution allows to utilize system capacity measure with a confidence and to evaluate the overall system performance. A measure for ergodic system capacity is established analytically through the mean value of the effective SINR. The proposed performance measure is attractive for the system level since it incorporates the L2S model used as a quality measure of a radio link. The simulation results carried out in specific mobility scenarios in 3GPP LTE downlink network verify the analytical results and show clear impact of mobility on the system capacity. In addition, fast and accurate rank adaptation method based on system level capacity is developed. It provides efficient and computationally simple procedure for adaptation to the varying channel conditions.

**Keywords** Performance analysis, Link-to-System interface, effective SINR, capacity**ISBN (printed)** 978-952-60-4753-9**ISBN (pdf)** 978-952-60-4754-6**ISSN-L** 1799-4934**ISSN (printed)** 1799-4934**ISSN (pdf)** 1799-4942**Location of publisher** Espoo**Location of printing** Helsinki**Year** 2012**Pages** 154**urn** <http://urn.fi/URN:ISBN:978-952-60-4754-6>



**Tekijä**

Alexandra Oborina

**Väitöskirjan nimi**

Mobiilin Langattoman MIMO-OFDM Järjestelmän Suorituskyvyn Analyysia: Työkaluja ja Tuloksia

**Julkaisija** Sähkötekniikan Korkeakoulu**Yksikkö** Signaalinkäsittelyn ja Akustiikan Laitos**Sarja** Aalto University publication series DOCTORAL DISSERTATIONS 110/2012**Tutkimusala** Signaalinkäsittely**Käsitteilyajankohdan pvm** 21.08.2012**Väitöspäivä** 21.09.2012**Julkaisuluvan myöntämispäivä** 21.08.2012 **Kieli** Englanti **Monografia** **Yhdistelmäväitöskirja (yhteenveto-osa + erillisartikkelit)****Tiivistelmä**

Monen antennin ja usean kantoaallon hyödyntämiseen perustuvien langattomien lähetystekniikoiden odotetaan saavuttavan korkeita tiedonsiirtonopeuksia, spektritehokkuutta, hyvän kantaman, sekä parantavan radioyhteyden luotettavuutta. Nämä ovat vaatimuksia uusissa langattomissa standardeissa, kuten 3GPP LTE (Long Term Evolution) sekä 3GPP LTE-Advanced järjestelmissä. Monikanavaisissa moniantenni (MIMO, Multiple-Input-Multiple-Output) järjestelmissä voidaan hyödyntää keilanmuodostusta (beamforming), tilan monimuotoisuutta (spatial diversity) sekä tilakanavointia (spatial multiplexing). Usean kantoaallon moduloiminen OFDM (Orthogonal Frequency Division Multiplexing) tekniikan avulla lisää spektritehokkuutta ja mahdollistaa yksinkertaistettujen lähetin-vastaanotin -rakenteiden hyödyntämisen laajakaistaisessa tietoliikenteessä.

MIMO-OFDM lähetystekniikka vaikuttaa niin fyysisen rajapinnan, järjestelmätason kuin radioresurssien hallinnankin (RRM, Radio Resource Management) suunnitteluun, sekä myös siirtolinkin ja järjestelmän väliseen L2S (Link-to-System) rajapintaan. Tässä väitöskirjassa kehitetään langattomien MIMO-OFDM järjestelmien L2S rajapinnan sekä RRM optimoimiseen soveltuvia menetelmiä, sekä järjestelmän suorituskyvyn arvioimiseen sopivia suorituskyvyn mittareita. Kehitetyillä menetelmillä voidaan analysoida langattomien verkkojen peittoaluetta, keskinäistä häiriötä, taajuuksien käyttöä sekä liikenteen tasapainotusta, joita tarvitaan verkon suunnitteluun ja optimoimiseen. Näitä menetelmiä käytetään lisäksi dynaamisissa järjestelmätason simulaatioissa.

Tässä työssä esitetään laskennallisesti tehokas menetelmä tehollisen signaali-häiriö-kohina suhteen (SINR, Signal-to-Interference-and-Noise-Ratio) laskentaan ja muuntamiseen MIMO-OFDM järjestelmän kehittyneelle L2S rajapinnalle. Lisäksi johdetaan tehollisen SINR arvon asymptoottinen jakauma. Nopean linkkien mukauttamisen ja adaptiivisen modulaation ja koodauksen tapauksessa mallinnukseen käytetään sekajakaumaa. Johdettu jakauma mahdollistaa järjestelmän kapasiteetin luotettavan arvioimisen ja käytön koko järjestelmän suorituskyvyn mittaamiseen. Tehollisen SINR keskiarvon avulla voidaan analyttisesti laskea järjestelmän ergodininen kapasiteetti. Kehitetty suorituskyvyn mittari soveltuu erityisen hyvin järjestelmätasolle, sillä sitä voidaan käyttää L2S mallin hyödyntämiseen radioyhteyden laadun analysoimiseen. Suoritetut simuloinnit tietyissä 3GPP LTE mobiiliverkon

**Avainsanat** Suorituskyvyn analysointi, L2S (Link-to-System) rajapinta, tehollinen SINR, kapasiteetti**ISBN (painettu)** 978-952-60-4753-9**ISBN (pdf)** 978-952-60-4754-6**ISSN-L** 1799-4934**ISSN (painettu)** 1799-4934**ISSN (pdf)** 1799-4942**Julkaisupaikka** Espoo**Painopaikka** Helsinki**Vuosi** 2012**Sivumäärä** 154**urn** <http://urn.fi/URN:ISBN:978-952-60-4754-6>





# Preface

The research work for this doctoral thesis was carried out at the Department of Signal Processing and Acoustics, School of Electrical Engineering, Aalto University (formerly Helsinki University of Technology), during the years 2006–2011. The work was done under the supervision of Academy Prof. Visa Koivunen, head of the Statistical Signal Processing group at the Department of Signal Processing and Acoustics, Aalto University, and principal investigator of SMARAD Centre of Excellence in Smart Radios and Wireless Research nominated by the Academy of Finland. The major part of the research work was done at first at Nokia Research Center and later at Nokia via Helsinki University of Technology.

I would like to express my gratitude to my supervisor, Prof. Visa Koivunen, for his tactful guidance during my studies and research work. His scientific advices have helped me to overcome many difficulties I encountered in my research work. It has been a great privilege to be supervised by and to work together with such an excellent researcher.

Further, I would like to thank all my co-workers, especially Martti Moisio and Tero Henttonen, with whom I co-authored several publications. The numerous discussions on the system level tools and models, their close guidance and fruitful cooperation have greatly contributed to my work. I would also like to thank Esa Pernila for the invaluable help in the simulator development.

I would like to thank my thesis pre-examiners, Prof. Tapani Ristaniemi and Dr. Samuli Visuri, for the effort they put to revise the thesis and for their comments and suggestions.

Furthermore, Prof. Ari Sihvola, the director of GETA Graduate School in Electronics, Telecommunications and Automation, and Marja Leppäharju, the GETA coordinator are highly acknowledged.

Special thanks go to Mirja Lemetyinen for assisting with all the practi-

cal issues, for polishing up my Finnish language skills and for bringing a warm and welcoming atmosphere into the lab.

I would like to thank all my colleagues in the department for the interesting discussions on many scientific and non-scientific aspects and for making the lab so pleasant place to work. Especially, I would like to acknowledge Mei Yen Cheong, Jan Oksanen, Tuomas Aittomäki, Sachin Chaudhari, Pekka Jänis, Jay Rajasekharan, Mário Costa, Taneli Riihonen, Karol Schober, Dr. Jussi Salmi, Dr. Traian Abrudan, Dr. Stefan Werner, Dr. Jan Eriksson, Prof. Andreas Richter, and Prof. Risto Wichman.

I would like to thank all my co-workers and colleagues at Nokia Research Center and Nokia. In particular, many thanks belong to Michal Hronec, Jani Puttonen, Jussi Ojala, Kennett Aschan, Elena Virtej, Markku Kuusela, Helka-Liina Määttänen, Dr. Timo Roman, Dr. Cássio Ribeiro, Dr. Klaus Hugel, Dr. Antti Sorri.

This research was funded by the GETA graduate school, Nokia Foundation grants and Nokia projects. I sincerely appreciate the financial support they provided during my studies.

I am deeply grateful to my parents and my sister for their support during all these years. Finally, and the most of all I would like to thank my husband Yaroslav and our kids Elizaveta and Theodor for bringing happiness into my life.

Espoo, August 7, 2012,

Alexandra Oborina

# Contents

<b>Preface</b>	<b>1</b>
<b>Contents</b>	<b>3</b>
<b>List of Publications</b>	<b>5</b>
<b>List of abbreviations</b>	<b>7</b>
<b>1 Introduction</b>	<b>11</b>
1.1 Motivation . . . . .	11
1.2 Scope of the thesis . . . . .	13
1.3 Structure of the thesis . . . . .	15
1.4 Summary of the publications . . . . .	15
<b>2 System model</b>	<b>19</b>
2.1 MIMO–OFDM system model . . . . .	19
2.2 Overview of MIMO performance gains . . . . .	20
2.3 MIMO techniques . . . . .	21
2.3.1 Beamforming . . . . .	21
2.3.2 Diversity . . . . .	22
2.3.3 Spatial multiplexing . . . . .	24
2.3.4 MIMO multiplexing diversity trade-off . . . . .	25
2.3.5 MIMO schemes in LTE DL . . . . .	26
<b>3 System Level Simulator</b>	<b>27</b>
3.1 Dynamic, static and semi–static simulators . . . . .	29
3.2 Simulator description . . . . .	31
3.3 Radio Resource Management . . . . .	32
3.3.1 Channel quality measurements . . . . .	33
3.3.2 Rank adaptation . . . . .	33

3.3.3	Scheduling . . . . .	34
3.3.4	Link adaptation . . . . .	36
3.3.5	Hybrid-ARQ . . . . .	37
3.3.6	Handover . . . . .	38
3.4	Simulation scenario . . . . .	39
3.5	Performance evaluation . . . . .	41
3.6	Discussion . . . . .	43
<b>4</b>	<b>Link-to-System Interface</b>	<b>47</b>
4.1	Traditional L2S interface . . . . .	49
4.2	Generic L2S interface . . . . .	51
4.3	Effective SINR mapping . . . . .	53
4.3.1	Calibration of the scaling parameter $\beta$ . . . . .	57
4.4	Comparison of effective SINR mappings . . . . .	58
4.5	EESM distribution . . . . .	61
4.6	Discussion . . . . .	62
<b>5</b>	<b>System capacity and performance evaluation</b>	<b>65</b>
5.1	MIMO capacity . . . . .	65
5.1.1	MIMO-OFDM capacity . . . . .	67
5.2	Rank adaptation using capacity approach . . . . .	68
5.3	Results on performance . . . . .	68
<b>6</b>	<b>Summary</b>	<b>73</b>
	<b>Bibliography</b>	<b>75</b>
	<b>Publications</b>	<b>87</b>

# List of Publications

This thesis consists of an overview and of the following publications which are referred to in the text by their Roman numerals.

**I** M. Moisio, A. Oborina. Comparison of Effective SINR Mapping with Traditional AVI Approach for Modeling Packet Error Rate in Multi-State Channel. *Lecture Notes in Computer Science*, vol. 4003/2006, pp. 461–473, June 2006.

**II** A. Oborina, M. Moisio, T. Henttonen, E. Pernila, V. Koivunen. MIMO Performance Evaluation in UTRAN Long Term Evolution Downlink. In *The 42nd Annual IEEE Conference on Information Sciences and Systems*, USA, Princeton, NJ, pp. 1179–1183, March 2008.

**III** A. Oborina, M. Moisio, V. Koivunen. Performance of Mobile MIMO OFDM Systems With Application to UTRAN LTE Downlink. *Accepted in IEEE Transactions on Wireless Communications*, In Press, to Appear in 2012.

**IV** A. Oborina, M. Moisio, V. Koivunen. Ergodic System Capacity of Mobile MIMO Systems using Adaptive Modulation. In *IEEE 21st International Symposium on Personal, Indoor and Mobile Radio Communications*, Turkey, Istanbul, pp. 2375–2380, September 2010.

**V** A. Oborina, V. Koivunen, T. Henttonen. Effective SINR Distribution in MIMO OFDM Systems. In *The Forty-Fourth Asilomar Conference on Systems, Signals and Computers*, USA, Pacific Grove, CA, pp. 511–515, November 2010.

**VI** A. Oborina, T. Henttonen, V. Koivunen, M. Moisio. Efficient Computation of Effective SINR. *46th Annual Conference on Information Sciences and Systems*, USA, Princeton, NJ, pp. 1–6, March 2012.

# List of abbreviations

3G	Third Generation
3GPP	Third Generation Partnership Project
4G	Fourth Generation
AcVI	Actual Value Interface
ARQ	Automatic Repeat reQuest
AVI	Average Value Interface
AWGN	Additive White Gaussian Noise
BLEP	Block Error Probability
BLER	Block Error Rate
BW	BandWidth
CDD	Cyclic Delay Diversity
CDF	Cumulative Distribution Function
CDMA	Code Division Multiple Access
CF	Central Frequency
CP	Cyclic Prefix
CPU	Central Processing Unit
CQI	Channel Quality Indicator
CSI	Channel State Information
DFT	Discrete Fourier Transform
EDGE	Enhanced Data rates for GSM Evolution
EESM	Exponential Effective SINR Mapping
eNB	evolved NodeB (base station)
ESM	Effective SINR Mapping
GSM	Global System for Mobile communications
HARQ	Hybrid-Automatic Repeat reQuest
HO	HandOver
IDFT	Inverse Discrete Fourier Transform
IEEE	Institute of Electrical and Electronics Engineers

ILLA	Inner Loop Link Adaptation
IRC	Interference Rejecting Combining
ISD	Inter-Site Distance
L2S	Link-to-System interface
LA	Link Adaptation
LTE	Long Term Evolution
LTE-A	Long Term Evolution-Advanced
LuT	Look-up Table
MCS	Modulation and Coding Scheme
MI-ESM	Mutual Information Effective SINR Mapping
MIMO	Multiple-Input Multiple-Output
MMSE	Minimum Mean-Square Error
MRC	Maximum Ratio Combining
MT	Mobile Terminal
MU-MIMO	Multi-User Multiple-Input Multiple-Output
OFDM	Orthogonal Frequency Division Multiplexing
OFDMA	Orthogonal Frequency Division Multiple Access
OLLA	Outer Loop Link Adaptation
PARC	Per Antenna Rate Control
pdf	Probability Density Function
PLoss	Penetration Loss
QAM	Quadrature Amplitude Modulation
QPSK	Quadrature Phase Shift Keying
QS	Quasi-Static
RRM	Radio Resource Management
RSRP	Reference Signal Received Power
RSRQ	Reference Signal Received Quality
RSSI	Received Signal Strength Indicator
SFBC	Space-Frequency Block Coding
SIMO	Single-Input Multiple-Output
SINR	Signal-to-Interference-plus-Noise Ratio
SISO	Single-Input Single-output
SLS	System Level Simulator
SNR	Signal-to-Noise Ratio
STTD	Space Time Transmit Diversity
SU-MIMO	Single-User Multiple-Input Multiple-Output
UMTS	Universal Mobile Telecommunications System
UTRAN	UMTS Terrestrial Radio Access Network



WiMAX	Worldwide Inter-operability for Microwave Access
WLAN	Wireless Local Area Network
WMAN	Wireless Metropolitan Area Network



# 1. Introduction

## 1.1 Motivation

Wireless communications have evolved very rapidly. The rapid growth in the number of new subscribers, the development of different global technologies and wireless standards, the demand in the new, better quality, low cost services as well as higher data rates are the main motivations for the evolution in the wireless communications.

The communication over wireless channel has three fundamental distinctions from the wireline communication [89,97]. First is the large-scale and small-scale fading, second is the interference between the transmitter-receiver pairs, and third is the user mobility in the network. The presence of fading, interference and mobility makes the design of wireless communication system challenging. The conventional design focusing on the reliability of the connection needs to mitigate the fading and multipath effects. Modern wireless system design focusing on the spectral efficiency gains from the rich multipath environment by means of utilizing spatial diversity through the Multiple-Input Multiple-Output (MIMO) communications. The MIMO system as a system with multiple antennas at the transmitter and the receiver theoretically allows linear growth of the link capacity. The capacity is proportional to the rank of MIMO channel [96]. While high spectral efficiency can be obtained through spatial multiplexing, many other MIMO system benefits such as improved signal quality and coverage can be achieved via spatial diversity, beamforming, space time coding and interference cancellation [36,97]. However, all the gains can not be achieved simultaneously due to their dependence on antenna configuration and scattering environment.

Multi-carrier modulation such as Orthogonal Frequency Division Multiplexing (OFDM) is currently the most prominent technology for spec-

trum efficient transmission. Since it is mitigating inter-symbol interference and enhancing system capacity, it is also well suitable for MIMO channel transmission. Furthermore, it facilitates using very simple equalization even in very broadband communications.

By combining MIMO system with OFDM technique the desired system requirements, such as good coverage in non-line-of-sight environment, reliable transmission, high peak data rates as well as high spectral efficiency, may be fulfilled [75, 85, 91]. Multi-stream multi-carrier wireless transmission has been already standardized in IEEE 802.11n WLAN, IEEE 802.16 WMAN, IEEE 802.16 WiMAX as well as in 3GPP Long Term Evolution (LTE) and it will be the key transmission technology for the future 4G broadband wireless communication networks.

The aspects of MIMO–OFDM technology, such as multi–antenna configuration, sub-carrier scheduling and optimization, large number of resource elements, need to be taken into account in the design of physical level, system level as well as interaction between link and system level called Link-to-System (L2S) interface. The evaluation of the quality of a radio link involving specific characteristics like spacial pre- and post-processing, synchronization, channel estimation, channel coding, modulation is done at a link level. The system level aims at evaluating the entire wireless network performance while taking into account terminal mobility, intercell interference, scheduling, handover, link adaptation in several typical deployment scenarios. The purpose of L2S interface is to determine the performance of radio link in terms of packet or block error rate in order to adapt transmission modes at the system level.

The system level requirement of accurately estimating the performance of each link using link level simulations in a reasonable time can not be fulfilled. Hence, there is a demand for a simple and efficient L2S interface model that accurately predicts link error probability for MIMO–OFDM system with a large number of frequency, time and space resource quality measures. The L2S interface model has to provide a system level quality measure, called effective Signal-to-Interference-and-Noise-Ratio (SINR), for link error prediction based on instantaneous channel and interference conditions. Additionally, the effective SINR can be used to evaluate the system level performance based on a capacity criterion and taking into account the impact of adaptive modulation and coding, Hybrid–Automatic Repeat reQuest (hybrid-ARQ, HARQ) and mobility.

On the system level MIMO–OFDM transmission influences the design

of many Radio Resource Management (RRM) functions and in particular dynamic rank adaptation. Rank adaptation is the procedure to adapt number of MIMO streams, for each user according to the rank of MIMO channel experienced by the mobile terminal [100]. Dynamic rank adaptation allows fast adaptation to varying channel conditions, and consequently, brings either MIMO multiplexing or diversity gains. The prediction of the transmission mode based on maximum total expected throughput is time demanding. More efficient rank adaptation algorithm achieving the same system performance is required to achieve MIMO multiplexing and diversity gains.

## 1.2 Scope of the thesis

The objective of this thesis is to develop methods for optimizing the L2S interface for multi-carrier multi-antenna wireless systems and to develop performance measures suitable for the system level performance evaluation. This thesis contributes to the development of beyond 3G and 4G broadband wireless communication networks. In particular, the developed techniques can be applied to fast and accurate performance evaluation of MIMO-OFDM transmission in the system level studies. System level performance studies are necessary to analyze such topics as coverage, interference, frequency utilization, traffic loading. Such quantitative results are required by standardization communities as well as mobile network operators for the network planning and optimization.

The first goal of this thesis is to develop optimized L2S interface in order to evaluate the performance at the system level in an accurate and numerically efficient manner. The comparison of traditional L2S interface [19,61,104] with effective SINR mapping methods studied in this thesis is needed to demonstrate the benefits and drawbacks of each method. A fast and accurate L2S interface approach for MIMO-OFDM system performance evaluation has to be developed. A computationally efficient method for calculating effective SINR is needed to reduce the CPU time of the system level simulations without any significant loss in the performance.

The second goal of the thesis is to develop a measure of performance for wireless communication systems suitable for the system level. The L2S interface model has to be incorporated into the performance mea-

sure, since the effective SINR is heavily used on the system level as a quality measure of a radio link. By establishing the distribution of effective SINR allows to utilize the performance measure with confidence in different scenarios and to analyze the impact of link adaptation and retransmissions on the performance.

Additionally, the problem of optimizing radio resource management and in particular rank adaptation is addressed in this thesis. The goal is to develop computationally efficient dynamic rank adaptation methods that provide speed up in CPU time without any loss in the system performance.

This thesis focuses on single-user MIMO mode in 3GPP LTE downlink network, as it is a baseline transmission method in 3GPP LTE. The performance studies are conducted by using analytical tools as well as fully dynamic system level simulations in realistic scenarios. The proposed algorithms can be used in the standardization process of next generation wireless communications in order to understand the expected performance of the system. This thesis contributes to the design and optimization of L2S interface and to the performance evaluation of multi-carrier multi-stream transmission on the system level. The contributions of the thesis are the following.

1. A comparison of advanced L2S interface approaches with the traditional L2S interface method is provided in order to highlight the main difference in prediction of multi-state channel performance.
2. A computationally efficient method for the effective SINR calculation is developed. The accuracy of fast calculation of the effective SINR is evaluated using analytical tools as well as system level simulations.
3. A system level performance measure based on the mean of the effective SINR is introduced.
4. The distribution of the effective SINR for uncorrelated and correlated cases is established using analytical methods. The knowledge of the distribution is applied to the ergodic capacity. It facilitates evaluating the impact of the link adaptation as well as retransmission to the system performance.
5. A rank adaptation algorithm is developed in order to optimize radio

resource management. The proposed rank adaptation provides the same performance as existing throughput-based rank adaptation procedure [103] at lower computational cost.

6. MIMO models as well as L2S interface functionality are implemented in a statistical simulator platform developed by Nokia Research Center and Nokia. The software development and the simulations evaluation required a significant effort. The simulator and the tools developed in this thesis have been successfully used in the standardization process of beyond 3G wireless communication network in 3GPP community. Moreover, the proposed algorithms are incorporated to the simulator platform.

### **1.3 Structure of the thesis**

This thesis consists of an introductory part and a collection of the six original publications. This introductory part of the thesis is organized as follows. Chapter 2 presents an overview of MIMO–OFDM systems and discusses the benefits that such systems can provide. Chapter 3 gives an overview of different approaches for the system level simulators and focuses on the dynamic System Level Simulator (SLS) tool used for performance evaluation in the publications of author. Chapter 4 presents the L2S interface methodology and describes the contribution of this thesis for the L2S interface optimization. Also, in this chapter, the effective SINR distribution is established and discussed. Chapter 5 discusses the capacity of MIMO–OFDM system and focuses on the ergodic capacity representation based on the effective SINR. The developed approaches for dynamic rank adaptation are summarized and the performance results of MIMO–OFDM transmission are illustrated. Chapter 6 summarizes the results and the contributions of the thesis.

### **1.4 Summary of the publications**

This section provides a summary of the original publications Publications I–VI and appended at the end of the manuscript starting from page 85.

The Publication I compares different L2S interface approaches in order to discriminate an impact on the final system performance and it proposes a preferred L2S mapping method for multi-carrier transmission. Additionally, an improvement of the traditional L2S interface method is proposed. The high accuracy of effective SINR mapping methods is demonstrated. As a result, exponential effective SINR mapping approach is later used as a baseline L2S interface method for a MIMO–OFDM transmission.

In Publication VI a computationally efficient method for calculating the effective SINR is developed. The proposed approach reduces the number of quality measures involved in the mapping without any significant loss in the system spectral efficiency. The accuracy of proposed approach is established analytically and verified by Block Error Rate (BLER) performance comparisons using system level simulations. The results show that the proposed algorithm is capable of accurately estimating the receiver performance for a MIMO–OFDM transmission and bringing significant reduction in the CPU time in system level simulations.

In Publication II a capacity-based rank adaptation algorithm is proposed. The algorithm allows for optimizing radio resource management. The proposed procedure is based on the maximum capacity over the whole bandwidth for a single or dual stream transmission. The simulation results show that the capacity-based rank adaptation has low complexity and is able to achieve similar performance compared to throughput-based adaptation [103]. Additionally, the effect of mobility to the system performance with multi-stream transmission is evaluated through the simulations in specific scenarios in 3GPP LTE downlink network.

In Publication III a system level performance measure based on the ergodic capacity for MIMO–OFDM system is proposed. A capacity expression is formulated through the mean value of the effective SINR in order to take into account L2S interface model, that is heavily used on the system level. The asymptotic distribution of the effective SINR is established analytically for uncorrelated and correlated cases. The mean value of the effective SINR is derived based on the moment generating function of post-processed SINR. It is used to provide an analytical form of the ergodic capacity. Additionally, the impact of mobility on the system performance is characterized through the ergodic capacity. The simulations carried out in specific mobility scenarios in 3GPP LTE downlink network verify the analytical results and show a clear impact of the mobility on



the system capacity.

In Publication IV the impact of adaptive modulation and hybrid-ARQ to the effective SINR as well as ergodic system capacity for OFDM-MIMO systems is established analytically and validated by simulations. The simulations carried out in specific mobility scenarios in 3GPP LTE downlink network show that link adaptation combined with retransmissions increases the performance, especially in low mobility case.

In Publication V the distribution of the effective SINR for the case of correlated post-processed SINR is established analytically and is verified by simulations using 3GPP LTE downlink network model. The knowledge of the distribution can be used for the ergodic capacity of MIMO-OFDM system in order to evaluate the performance on the system level.

The algorithms proposed by the author have been modeled and implemented in the statistical simulator platform developed in Nokia Research Center and Nokia. The simulator and the obtained results are known to the 3GPP community via standardization contributions. The quality and reliability of the simulator and the results are proven and approved through the 3GPP system level evaluation contributions in the technical specification group Radio Access Networks [2].

In publications Publication II, Publication III, Publication IV, Publication V, Publication VI the original idea is developed by the first author. All the derivations and simulations and post-processing of the results were performed by the first author as well. In Publication I the authors are listed in the alphabetical order. In the publication Publication I the original idea is developed by the second author as well as derivations and the simulations. The co-authors provided the guidance in the theoretical modeling, in the design of the experiments and helped in writing the papers.



## 2. System model

This chapter gives a brief overview of MIMO wireless communication technology in combination with OFDM (MIMO–OFDM) as a transmission method for the mobile cellular wireless network. The main objective is to provide a formal description of system model employed throughout this thesis. The model facilitates describing the transmission methods used in 3GPP LTE wireless network.

### 2.1 MIMO–OFDM system model

OFDM modulation with  $K$  sub-carriers turns a broadband wireless channel into a set of frequency flat MIMO channels. A MIMO–OFDM system model with  $N_t$  transmit antennas and  $N_r$  receive antennas can be formulated for each sub-carrier as follows

$$\mathbf{y}_k = \mathbf{H}_k \mathbf{W}_k \mathbf{s}_k + \mathbf{n}_k, \quad (2.1)$$

$N_r \times 1$     $N_r \times N_t$     $N_t \times N_s$     $N_s \times 1$     $N_r \times 1$

where vector  $\mathbf{y}_k$  is the received signal at  $k$ -th sub-carrier, matrix  $\mathbf{H}_k$  represents the channel response, vector  $\mathbf{s}_k$  contains the transmitted symbols with power constraint  $E(\mathbf{s}_k \mathbf{s}_k^H) = \frac{P}{N_s} \mathbf{I}_{N_s}$ ,  $P$  is the total transmitted power,  $N_s \leq \min(N_t, N_r)$  is the channel rank that represents the number of spatially multiplexed data streams. Matrix  $\mathbf{W}_k$  is a precoder. Throughout this thesis a unitary precoder [5] satisfying transmit constraints  $\mathbf{W}_k^H \mathbf{W}_k = \mathbf{I}_{N_s}$  is used. Vector  $\mathbf{n}_k$  contains the additive white Gaussian noise and inter-cell interference and is assumed to be zero-mean Gaussian with covariance  $E(\mathbf{n}_k \mathbf{n}_k^H) = \mathbf{R}_k$ . Here, subscript  $(\cdot)^H$  stands for hermitian transpose.

A MIMO–OFDM block transmission scheme is illustrated in Figure 2.1 with single OFDM modulator used per transmit antenna.

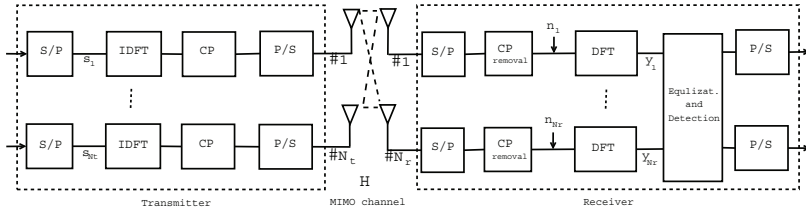


**Figure 2.1.** MIMO-OFDM system with  $N_t$  transmit antennas and  $N_r$  receive antennas for MIMO channel.

Inverse Discrete Fourier Transform (IDFT) as a part of modulation process and Discrete Fourier Transform (DFT) as a part of demodulation process of OFDM may be computationally efficiently realized by fast Fourier Transform algorithm.

In the 3GPP LTE physical layer specification [5] OFDM is chosen as basic modulation scheme in downlink and is accomplished by OFDMA as a user-multiplexing access scheme. The OFDMA multiple access is beneficial in the following aspects: high data rate and high spectral efficiency in frequency selective fading channels, low receiver complexity, bandwidth scalability. It facilitates frequency domain scheduling and link adaptation as well as enabling MIMO transmission with accurate use of channel state information [46]. But OFDMA also imposes some challenges to transceiver designers such as sensitivity to synchronization errors, i.e., carrier frequency offset, and high peak-to-average power ratios.

## 2.2 Overview of MIMO performance gains

The use of multiple antennas in the receiver and/or in the transmitter basically provides the following advantages.

- **Array gain.** Array gain is an increase in average received SNR obtained by coherently combined signals transmitted from multiple antennas or received by multiple antennas. In order to get array gain channel knowledge at the transmitter or receiver is required.
- **Diversity gain.** Diversity gain refers to improved link reliability in space, time, frequency or polarization. Diversity gain can be exploited in the case of independently fading multiple channels experienced by different antennas in order to mitigate the effect of multipath fading. Diversity gain is expressed in terms of order, which is characterized by

the slope of error probability performance curve.

- **Spatial multiplexing gain.** Multiplexing gain corresponds to the increased data rate due to the ability to transmit multiple parallel data streams over MIMO channel without increasing the bandwidth or total transmit power. The capability to support multiple streams depends on the rank of the channel matrix  $\mathbf{H}$ .

As a result, the MIMO technology can be used to achieve improved system performance, such as increased spectral efficiency, increased user throughput, better coverage. In general it is not possible to exploit all these gains provided by MIMO technology simultaneously due to conflicting demands on the spatial degrees of freedom (or number of antennas) [75].

3GPP LTE standard is the first global mobile cellular system where MIMO as a key technology is initially included in the standard development [88]. Two different concepts can be distinguished between multiple antenna techniques: Single-User MIMO (SU-MIMO) and Multi-User MIMO (MU-MIMO). SU-MIMO is the conventional point-to-point MIMO system between the base station and the mobile station, while MU-MIMO is a virtual MIMO communication link, where MIMO channel is created between the base station and several mobile stations sharing the same frequency and time domain resources. SU-MIMO is the dominant technology for LTE downlink transmission and in the thesis we focus only on it.

## 2.3 MIMO techniques

In this section the benefits of multiple antenna usage are briefly reviewed. Then different categories of MIMO transmission techniques adopted in 3GPP LTE Release 8 and used in the publications of author are discussed.

### 2.3.1 Beamforming

Beamforming techniques are designed to transmit or receive the signal to/from the preferred directions, where multiple antennas are used to shape the overall antenna beam in a certain way in order to maximize antenna gain in target direction or to suppress target dominant interfer-

ence [23]. The main goal of beamforming is to increase received signal power and, subsequently, to improve coverage.

For the receiver beamforming case ( $N_t = 1, N_r > 1$ ) the received signal can be optimally linearly combined from different receive antennas in order to maximize the received SINR. The mean received SINR can be increased proportionally to  $N_r$  and array gain of  $10 \log_{10}(N_r)$  dB over the single antenna case can be exploited. Channel State Information (CSI) at the receiver is typically available.

For the transmit beamforming case ( $N_t > 1, N_r = 1$ ) CSI is required and can be obtained from feedback. The transmit beamformer based on perfect channel information can be designed to maximize the received SINR. The average received SINR can be increased proportionally to  $N_t$  and array gain of  $10 \log_{10}(N_t)$  dB over the single antenna case can be exploited.

For the beamforming a high antenna correlation caused by small inter-antenna distance is beneficial in order to provide array gain. In this case the channels between different transmit antennas and receiver are highly correlated meaning having the same fading. And these channels differ only in the phase component. Therefore, applying specific phase shifts at different antennas power can be steered to the desired direction [23]. For the low antenna correlation scenario beamforming is also possible if fast feedback information is available. In this case the transmit beamformer is a precoder. It consists of complex weights and is chosen from the pre-defined codebook in order to steer the beam and to compensate against fading. The precoding provides beamforming gain and additionally diversity gain.

An overview of beamforming techniques can be found in [23,25,88]. Precoding techniques are specifically discussed in [47].

### 2.3.2 Diversity

The goal of diversity oriented techniques is to provide robustness against fading by same signal transmission over multiple independently fading paths. There are different potential sources of diversity, such as space, time, frequency or polarization.

Full spatial diversity with order of  $N_t N_r$  can be obtained if all  $N_t N_r$  independently faded links of MIMO channel are properly combined. In order to maximize diversity gain low antenna correlation is required, that can be achieved by large inter-antenna distance or by cross-polarization. Ad-

ditionally, diversity gain is accomplished by array gain obtained in all receiver combining diversity schemes and in the transmit diversity schemes with available CSI.

In receiver diversity independent fading paths from different receive antennas are combined at the receiver to mitigate the effect of fading. Linear and non-linear combining at the receiver with spatial domain processing can be designed to maximize the post-processed SINR or to suppress specific interferers. Maximum Ratio Combining (MRC) [38] combines the signals from different receive antennas with weights proportional to channel gains

$$\mathbf{G}_k^{(\text{MRC})} = \tilde{\mathbf{H}}_k^H, \quad (2.2)$$

where  $\tilde{\mathbf{H}}_k = \mathbf{H}_k \mathbf{W}_k$ .

As a result, the SINR is increased after MRC. MRC receiver is preferable in noise dominating scenario with relatively large number of interfering signals. In the interfering dominant scenarios the Interference Rejecting Combining (IRC) [15, 106] as a linear receiver is beneficial to suppress the dominant interference.

$$\mathbf{G}_k^{(\text{IRC})} = \tilde{\mathbf{H}}_k^H \mathbf{R}_k^{-1} \quad (2.3)$$

In the general case with  $N_t > 1, N_r > 1$  the Minimum Mean Square Error (MMSE) [38, 54] receiver, that minimizes the average mean square error  $E(\|\mathbf{G}\mathbf{y} - \mathbf{s}\|_F^2)$ , can be designed in order to optimally combine and balance between the multi-stream interference mitigation and noise enhancement.

$$\mathbf{G}_k^{(\text{MMSE})} = \tilde{\mathbf{H}}_k^H \left( \tilde{\mathbf{H}}_k \tilde{\mathbf{H}}_k^H + \mathbf{R}_k \frac{N_s}{P} \right)^{-1} \quad (2.4)$$

Transmit diversity can be exploited from different diversity oriented techniques in order to increase frequency or time selectivity and, as a result, to stabilize the received signal power in fading channel. Here we discuss the space-time coding, space-frequency coding and delay diversity schemes used in LTE. These schemes do not require CSI at the transmitter.

Space-time block coding scheme called Space Time Transmit Diversity (STTD) maps the modulation signals orthogonally according to Alamouti coding [9] in time for each antenna pair to capture the transmit diversity and to provide robustness against fading. Orthogonality allows to recover transmitted symbols with linear receiver without interference. Space-Frequency Block Coding (SFBC) can be considered as frequency domain adaptation of space-time block coding, where Alamouti coding is applied

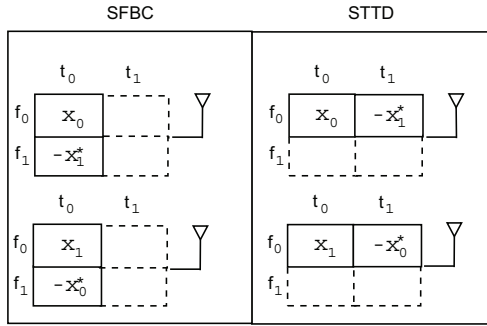


**Figure 2.2.** Transmit diversity schemes: STTD and SFBC.

in frequency for each antenna pair. The STTD and SFBC schemes for 2 transmit antennas are illustrated in Figure 2.2. The main drawback of STTD and SFBC that optimum code, i.e., orthogonal with rate of one, can be achieved only for 2x1 MIMO channel with full transmit diversity [23, 92].

The delay diversity can be achieved by transmitting the signal through different transmit antenna with different delay. Adding a time delay is identical to applying a phase shift in the frequency domain. As a result, virtual multipath is created and spatial diversity is transformed to the frequency diversity. Thus, increased frequency diversity is achieved. In OFDM transmission it is realized by Cyclic Delay Diversity (CDD) scheme [48].

### 2.3.3 Spatial multiplexing

As discussed earlier in section 2.3.1 and section 2.3.2 multiple antennas technique can be used to increase received Signal-to-Noise-Ratio (SNR) and/or to exploit diversity against fading. The Modulation and Coding Scheme (MCS) adaptively combined with such beamforming or diversity method can indirectly lead to the increased data rate. However, the multiple antennas at both transmitter and receiver ends can directly be utilized to increase significantly the data rate through spatial multiplexing [107], [33, 96]. Spatial multiplexing allows to transmit at most  $\min(N_t, N_r)$  different data streams in parallel in case of good channel conditions (high SINR regime, rich multipath propagation, uncorrelated antennas) [107], [76], [33, 96]. The number of spatially multiplexing streams can be determined as a rank of MIMO channel matrix  $H$ .

In open-loop MIMO case with no available CSI the Maximum Likelihood



receiver can provide near-capacity performance [23]. However, the high receiver complexity for large MIMO system makes it unusable. The reduced complexity receivers, such as MMSE with Successive Interference Cancellation [99] for multi-codeblock transmission can achieve almost the same performance [56]. The transmitted codeblock can contain several multiplexing streams and can be combined with individual link adaptation mechanism (Per Antenna Rate Control (PARC) [40]).

In close-loop MIMO case with available CSI beamforming and spatial multiplexing can be combined by means of precoding based spatial multiplexing. If full CSI is available the orthogonal precoding allows to make orthogonal spatial multiplexing streams and to remove inter-stream interference at the receiver. Orthogonal precoding can be designed using singular value decomposition of the MIMO channel  $\mathbf{H} = \mathbf{U}\Sigma\mathbf{V}^H$  with transmit precoder denoted by  $\mathbf{V}$  and receiver shaping by  $\mathbf{U}^H$ . As a result, the MIMO transmission can be decomposed into parallel orthogonal streams according to eigenmodes of the channel.

Due to limited feedback information perfect CSI is usually not available in the modern wireless networks. The suitable precoding vector is found on the receiver side from the known codebook based on the specified criteria, i.e., maximizing the instantaneous received SINR or maximizing the throughput.

### 2.3.4 MIMO multiplexing diversity trade-off

As discussed above MIMO system can provide two types of gains over SISO system: spatial multiplexing gain  $r_m$  and diversity gain  $d$  with extreme values at high SNR to be equal  $r_m = \min(N_t, N_r)$  at fixed error rate and  $d = N_t N_r$  at fixed transmission rate.

Usually the transmission schemes are designed to extract either spatial multiplexing gain or diversity gain. However, desiring to utilize an increase in SNR for combination in transmission rate increase and error rate reduction the fundamental trade-off has been found [97]. For a given MIMO channel both gains can be simultaneously obtained, but there is a following trade-off how much any coding scheme can get of each type of gain [108]

$$d(r_m) = (N_t - r_m)(N_r - r_m). \quad (2.5)$$

This trade-off implies that out of total resources of  $N_t$  transmit antennas and  $N_r$  receive antennas, if  $r_m$  transmit antennas and  $r_m$  receive anten-

nas are used for spatial multiplexing the remaining  $N_t - r_m$  transmit and  $N_r - r_m$  receive antennas provide diversity. Thus, adding one more transmit and one more receive antenna, the spatial multiplexing gain can be increased by one while the scheme is keeping the same diversity order.

### 2.3.5 MIMO schemes in LTE DL

In 3GPP LTE DL network the following schemes are used in the publications of author:

- Open-loop MIMO rank 1 transmission: transmit diversity scheme (CDD-like, SFBC) with MRC or IRC receiver,
- Open-loop MIMO rank 2 transmission: spatial multiplexing(PARC) with MMSE receiver,
- Close-loop MIMO rank 1 transmission: DFT precoding based transmission with MRC or IRC receiver,
- Close-loop MIMO rank 2 transmission: DFT precoding based spatial multiplexing with MMSE receiver.

Open-loop MIMO schemes can be used in downlink if only partial feedback information is available at the base station. The mobile station reports the channel rank only but no precoding information. Depending on MIMO channel conditions, i.e., rank information, base station scheduler can select the number of spatial streams used for spatial multiplexing. In the case of rank 1 transmission transmit diversity schemes can be used, otherwise spatial multiplexing scheme can be utilized. Close-loop MIMO schemes can be used if available feedback information consists of rank information and index of preferred precoding matrix. In the case of rank 1 close-loop MIMO transmission transmit diversity and beamforming gains can be exploited. With a higher rank transmission, both beamforming and spatial multiplexing gains can be achieved.

Obviously, all the benefits of multiple antenna usage can not be achieved simultaneously. The transmission scheme and transceiver design determine the exploited gains of MIMO technology.

### 3. System Level Simulator

In order to study topics related to the network planning and optimization of future wireless communications, such as coverage, interference analysis, frequency utilization, traffic loading, etc., system level performance evaluations are required by standardization communities as well as mobile network operators.

Performance evaluation of wireless networks by simulations is widely used for the research and development purposes due to the following benefits [51].

1. Systems have so many parameters and degrees of freedom that studying performance using analytical tools may be impossible or extremely tedious.
2. The performance evaluation can be done fast at low cost of modeling new algorithms and controlling the experiments.
3. Computer simulations allow the evaluation of future systems that are not yet deployed or still under development or standardization.
4. The environment including propagation, traffic, layout conditions and other parameters is fully controlled and transparent. So, the parameters that impact on the performance can be discovered.
5. Simulation results can be repeated if the same parameters are utilized. That makes the comparison of concepts feasible.

The simulations can not provide perfect performance evaluation due to simplifications made in modeling of wireless environment. However, with the help of computer simulations the limits in the system performance can be identified. Moreover, accurate and controlled comparison in perfor-

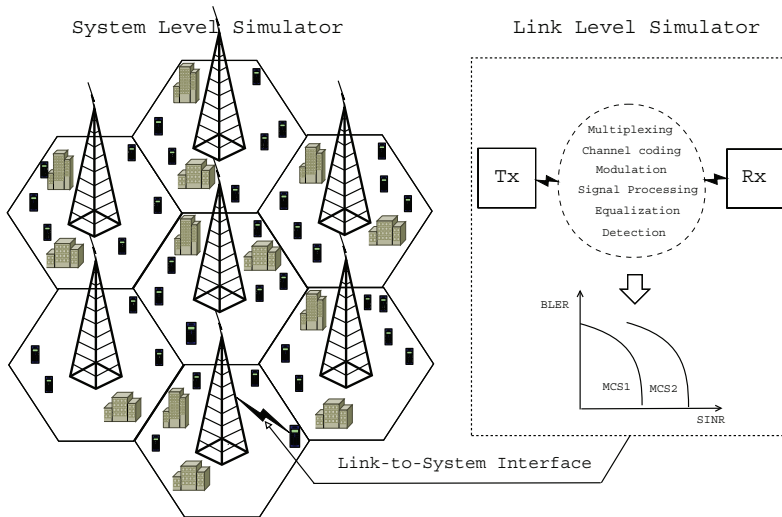


**Figure 3.1.** Two level architecture for simulations of wireless networks.

mances of different systems can be made by means of the simulations.

Due to complexity reasons a single simulator to model entire wireless communication system with all functionality is not feasible. Thus, two level architecture consisting of link level simulator and system level simulator [10, 55] has been adopted for analyzing, testing and evaluating wireless network behavior. The goal of the link level simulator is to estimate the quality of a specific link between transmitter and receiver under different channel propagation conditions. Also performance of a specific transmitter–receiver configuration can be studied by means of the link level simulator. The goal of the system level simulator is to evaluate the performance of the whole network in terms of capacity, coverage or the behavior of a radio resource management. The estimation of the quality of the connections on the system level is simplified and the outcome of the link level simulations is used here. The link level and the system level simulators interact with each other by means of Link-to-System interface. Figure 3.1 illustrates the concept of two level architecture for computer simulations.

Additional reasons of two level architecture for performance evaluation are the following. Performance gains achieved at the link level are not necessarily translated to the corresponding gains at the system level as claimed in [8]. Hence, there is a demand for the system level simulations in order to understand and learn the real performance gains.

The system level simulator is a tool for investigating the algorithms that can fully exploit the network capabilities. The system simulator can

be used to analyze the system characteristics such as mobility, traffic and optimized radio resource management algorithms. The system simulator can support network planning in optimization and tuning network parameters.

The dynamic SLS developed by Nokia for LTE performance evaluation yields the results that contributed into the 3GPP standard development [1]. The author has been involved in the simulator development as well as organizing simulations' campaigns for 3GPP standardization purposes. All the concepts and solutions proposed in the publications presented in the scope of this thesis have been evaluated by means of the system level simulations.

In this chapter the structure, properties and performance measures of the system simulator are considered. In section 3.1 system simulators with different simulation paradigm are introduced. The functionality of Radio Resource Management is presented in section 3.3. The simulation scenario and main parameters utilized for system level simulations are described in section 3.4. The performance measures on the system level as well as performance results for LTE network obtained by means of system level simulations are presented in section 3.5.

### 3.1 Dynamic, static and semi-static simulators

Unexpected problems experienced by real operating wireless networks such as parallel downloading by many subscribers football video could not be identified and solved by conventional static simulation tool as explained in [62]. The packet-switched data having high dynamic behavior can causes a "busy minute" problems whereas the static simulations estimates a "busy hour" performances. Additionally, the traffic, scheduling and mobility models require higher time resolution for proper analyzes, for example  $t \approx 10^{-3}$  sec. The time resolution provided by the static simulator is typically  $t \approx 10^0$  sec., and may also be significantly longer. Therefore, the dynamic simulations are desired to evaluate the real network performance with system parameters varying faster than a second.

The most appropriate classification of the simulators is presented in [22, 24, 62] and can be described as follows. The system simulators can be divided into three main categories: static, semi-static and dynamic. The category is formed depending on how the air interface, user mobility and

related algorithms evolve over time.

Static system level simulator [101] models the network at a single moment of time, called snapshot. During each snapshot mobile terminals are uniformly spread over the simulation area and do not change their positions. The pathloss and shadowing profiles are calculated for each active radio link based on the chosen propagation model and kept constant within a snapshot. Some RRM algorithms, e.g. power control, can have several iterations within a snapshots in order to achieve a solution close to a steady-state solution of optimal resource allocation. The independent snapshots of the performance are collected. Finally, the average performance of the simulated network is obtained using Monte Carlo method. The static simulations are fast, but due to independence of the snapshots the evaluation of RRM over time is not possible. The results of static simulations are applied for the capacity and coverage determination in the initial deployment and for validation of network optimization.

Dynamic system level simulator [24, 42] models behavior of mobile network for the whole simulation time period in a time driven manner. The time evolves with the discrete steps of predefined length. In the dynamic simulator the state in any time step is highly correlated with the state established in the preceding time steps. The movement of mobile terminals in the simulation area is explicitly modeled. The pathloss, shadowing and fast fading are continuously updated depending on the mobile terminal position. Detailed RRM algorithms are continuously performed according to the changing conditions of the radio channel. The simulation duration should be sufficiently long, typically million of steps, in order to provide the required confidence of the results and to obtain the effect of time correlation. The results of dynamic simulations are used for evaluation performance of RRM, and for measuring the impact of dynamic effects (user mobility, handover, system delays, traffic load) on the system performance, such as coverage and capacity.

The characteristics of both dynamic and static simulators are combined in semi-static simulators [62]. The main drawback of dynamic simulations is very long computational time. In order to reduce the computational load while taking into account the effect of mobility, at least partly, semi-static simulations may be carried out. The behavior of mobile stations is dynamically simulated for several time steps with detailed RRM within a snapshot. During the snapshot mobile terminals do not change their positions. The pathloss and shadowing profiles are calculated and

kept constant during the snapshot. The fast fading is modeled according to the mobile speed and involving the specific channel model. The results of semi-static simulations are used for analyzing RRM algorithms performance as well as multi-antenna strategies, but the dynamic effects such as handover and different traffic load can only be partly evaluated using semi-static simulations.

In Table 3.1 a comparison between static, semi-static and dynamic system level simulators is presented. Key properties such as mobility of Mobile Terminals (MT) and performance under RRM and HandOvers (HO) are considered.

### 3.2 Simulator description

The performance evaluation of mobile networks shown in publications Publications I–VI has been done using dynamic system level simulator. A flowchart of the operations performed by the dynamic system level simulator is illustrated in Figure 3.2.

During the initialization stage the simulation environment including cellular model, propagation model, base station network topology, uniformly spread mobile terminals, is created based on the provided input simulation parameters. During the simulation loop a single time step at the system level control in all network elements is executed. The simula-

**Table 3.1.** Comparison between static, semi-static and dynamic system level simulators.

<b>Properties of SLS</b>	<b>static</b>	<b>semi-static</b>	<b>dynamic</b>
Time driven behavior	no	partly	fully
Mobility of MT	stationary	stationary	modeled explicitly
Channel response	independent of mobile speed	dependent on mobile speed	dependent on mobile speed
<b>Performance of SLS</b>	<b>static</b>	<b>semi-static</b>	<b>dynamic</b>
RRM evaluation	possible for simplified RRM	possible	possible
HO evaluation	impossible	possible for simplified HO	possible
Traffic evaluation	possible for full buffer	possible for full buffer	possible for any traffic

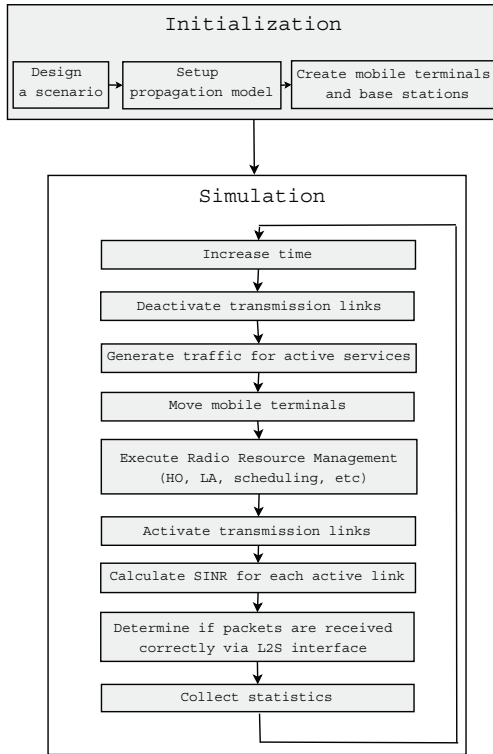


**Figure 3.2.** Simulation setup and main loop of dynamic system level simulator.

tion loop aims at determining the success or failure of a packet transmission for each active link in order to collect the performance statistics.

The simulator output is a collection of different statistical results obtained during the simulation run from the central cells only in order to avoid distorting edge effects. The examples of packet-wise statistical results are post-processed SINR, chosen MCS, rank of the transmission, success of the transmission and packet delay. Examples of station-wise statistical results are an average throughput over predefined period, an average user load at base stations, number of handovers, number of dropped connections. In the simulator also the overall system spectral efficiency is collected.

### 3.3 Radio Resource Management

Radio Resource Management is a system level control of radio transmission characteristics in wireless communication systems. The objective of RRM is to utilize the limited radio resources in the network as efficient as



possible. RRM advanced functionality helps to achieve ambitious goals of future wireless networks.

In this chapter we only focus on the Channel Quality Indicator (CQI) manager, rank adaptation, scheduling, link adaptation, HARQ and handover, that have been used in the publications of author.

### 3.3.1 Channel quality measurements

The CQI measurements are computed by mobile terminals for either whole bandwidth or sub-bands with minimum resolution of 180 kHz, i.e., one Physical Resource Block. CQI provides the channel state information in terms of SINR as follows [57]

$$\text{SINR}_{\text{dB}}(n) = 10 \log_{10}(\text{SINR}_{\text{lin}}(n)) + \text{Error}_{\text{dB}}, \quad (3.1)$$

$$\text{CQI}_{\text{dB}}(n) = \text{QStep}_{\text{dB}} \text{floor} \left( \frac{\text{SINR}_{\text{dB}}(n)}{\text{QStep}_{\text{dB}}} + 0.5 \right). \quad (3.2)$$

First, linear SINR value is calculated for each resource element  $n$  based on received reference symbol power and total interference for every measurement period. Then linear SINR is converted to dB scale with a measurement error (zero mean Gaussian distributed random variable with a specified variance). CQI value can be obtained through the quantization with predefined quantization step length. Finally, the CQI measurements are reported to the base station (eNB) with a certain delay according to a specific reporting scheme, e.g. given in [57].

### 3.3.2 Rank adaptation

Rank adaptation is the procedure to adapt the transmission rank, i.e., number of MIMO streams, for each user according to the rank of MIMO channel experienced by the mobile terminal [100]. The rank of multi-stream transmission can be adapted up to  $\min(N_t, N_r)$  for  $N_t \times N_r$  MIMO system, but for the users experiencing poor propagation conditions a low rank transmission is preferable.

The rank adaptation consists of two stages. First, at the receiver side the transmission rank and an index of the best suitable precoding matrix (in case of close-loop MIMO mode) are estimated over the whole bandwidth and sent to the base station as a part of a CQI report. Frequency non-selective feedback about the precoding matrix does not provide full benefits of precoding [37, 78, 83], but it is chosen in order to reduce the simulation complexity and due to practical limitations of the amount of

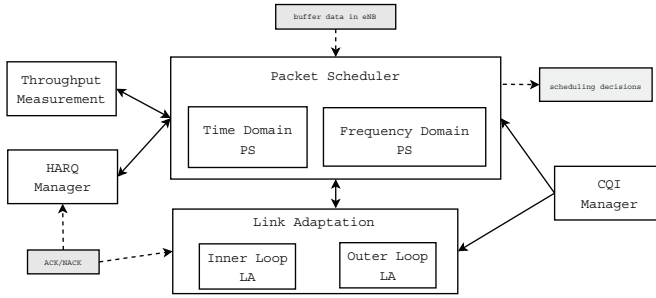


**Figure 3.3.** Packet scheduling framework in dynamic system level simulator.

feedback information.

The single CQI or multiple CQIs per resource block are reported to the base station depending on the selected rank. The selection criteria for the transmission rank and precoding matrix can be chosen in several ways leading to different computational complexity and performance as shown in Publication II, [58, 100]. The most preferred approach presented in [58] is to select the rank and precoding matrix according to the maximum estimated instantaneous throughput for all possible ranks and precoding matrix combinations.

At last, the base station makes the final decision about the rank for the next MIMO transmission based on the received feedback report.

### 3.3.3 Scheduling

Dynamic packet scheduler allocates the physical resources in frequency and time to the appropriate users based on user channel conditions. Packet scheduler closely cooperates with link adaptation, Channel Quality Indicator manager, throughput measurement and HARQ as shown in Figure 3.3 [52]. In order to rapidly adapt to the changing channel conditions packet scheduler, throughput measurement, link adaptation as well as HARQ manager are located at the base station.

According to [46,52,80] packet scheduling consists of two stages of scheduling process: time domain packet scheduling and frequency domain packet scheduling.

First, time domain scheduler select a subset of users based on largest calculated priority metric. Different priority metrics can be utilized. The priority metrics are evaluated via CQI averaged over the whole band, since the actual resource allocation does not occur in the time domain. The time domain scheduler considers both new transmissions and pend-

ing HARQ retransmissions. The prioritization of users with HARQ retransmissions has been employed in the simulations for all publications of author.

Next, the resources in the frequency domain are allocated to the candidates selected by time domain scheduler. Frequency domain scheduler does not guarantee that the resources will be allocated to all candidates. Scheduled user can have any number of allocated resources spread out in the frequency.

According to [52, 80] two different strategies are available in frequency domain scheduling: "Per-User" and "Per-Resource". If scheduler operates in "Per-User" mode, then candidates are prioritized by a specific priority metric, and the resources are scheduled to the most preferable candidate in turn until complete satisfaction of his needs is achieved. If scheduler operates in "Per-Resource" mode, then each resource element is allocated to the best candidates according to a priority metric.

Finally, when all resources are allocated, link adaptation manager selects the best possible MCS to each scheduled user based on feedback reports. And the decisions are provided to the physical layer at the base station.

Different scheduling algorithms lead to different system efficiency, such as throughput and spectral efficiency, and different user satisfaction, such as fairness. Comparing the system efficiency and user satisfaction the schedulers that are used in the publications are discussed next.

A scheduling algorithm can be formulated as utility-based optimization problem, that provides the user to have resources  $k$  with maximum scheduling priority metric  $P_{n,k}$

$$P_{n,k} = \frac{\hat{r}_n(k)^a}{\bar{R}_n^b}, \quad (3.3)$$

where  $\hat{r}_n(k)$  is expected instantaneous throughput for the scheduling resources  $k$  for user  $n$ ,  $\bar{R}_n$  is estimated average throughput experienced by user  $n$  before the pending scheduling,  $a$  and  $b$  are scalar coefficients. The coefficients  $a$  and  $b$  are chosen to achieve a trade-off between the desired user satisfaction and desired system efficiency.

In order to obtain the highest possible spectral efficiency, the scalar coefficients of scheduling algorithm should be  $a = 1$  and  $b = 0$ . As a result, the cell Maximum Throughput (or Maximum C/I) scheduler [23] is designed with priority metric  $P_{n,k}$

$$P_{n,k} = \hat{r}_n(k). \quad (3.4)$$

The scheduler serves the users with maximum CQI value, and hence, the highest possible cell throughput and spectral efficiency can be achieved. But the main drawback of the scheduler is fairness. The scheduler is unfair, since the users under bad propagation conditions are the least likely to be scheduled. Thus, the users that are located closer to the base station are prioritized by the scheduler.

In order to improve the fairness of the maximum throughput scheduler, the Proportional Throughput scheduler [23] takes the estimated average throughput into account. The Proportional Fair utilizes the priority metric

$$P_{n,k} = \frac{\hat{r}_n(k)}{R_n}. \quad (3.5)$$

Here scalar coefficients are designed to be equal, i.e.  $a = 1$  and  $b = 1$ . The past user throughput is estimated using throughput measurements as follows [52]

$$\overline{R}_n = (1 - \alpha)\overline{R}_{n-1} + \alpha\hat{r}_{n-1}, \quad (3.6)$$

where scalar  $\alpha$  evaluates importance of past information. The Proportional Fair scheduler balances the system efficiency and long term user satisfaction as shown in [52].

The fair scheduler with equal service quality is provided by Round Robin scheduler [23] with the following priority metric

$$P_{n,k} = \frac{1}{R_n}. \quad (3.7)$$

The scalar coefficients in this case are  $a = 0$  and  $b = 1$ . The scheduler gives the priority to the user with minimum data rate that has been waiting for a long time. The scheduler does not take into account the channel conditions experienced by the user.

### 3.3.4 Link adaptation

The link adaptation determines an appropriate MCS for each user based on a CQI feedback. The objective of link adaptation is to adapt fast to the changing propagation conditions experienced by the user for optimal utilization of the resources.

The link adaptation is performed at base station in order to adjust the transmitted bit rate on each time step. The link adaptation algorithm consists of two parts: Inner Loop Link Adaptation (ILLA) and Outer Loop Link Adaptation (OLLA) [46, 77, 78].

An OLLA [77] is the control algorithm that stabilize the BLER performance. The CQI values do not fully describe the channel conditions, they are erroneous and delayed due to measurement, quantization errors and report delaying. Therefore, OLLA algorithm is applied to correct the received CQI values in order to guarantee that the BLER of the first transmission does not exceed the parameterized target BLER. Thus, OLLA controls the BLER to be kept on the target level.

The OLLA adjusts each received user and resource unit specific CQI value with the offset as follows. The offset is decreased by  $\Delta_{\text{down}}$  dB for the successfully received packet. The offset is increased by  $\Delta_{\text{up}}$  dB for unsuccessfully received packet.

Using OLLA, the BLER of the first transmission converges to [77]

$$\text{BLER} = \frac{1}{1 + \frac{\Delta_{\text{up}}}{\Delta_{\text{down}}}}. \quad (3.8)$$

Thus, by selecting the ratio between  $\Delta_{\text{up}}$  and  $\Delta_{\text{down}}$ , the BLER target for the first transmission can be controlled [77]. The value of  $\Delta_{\text{down}}$  can be calculated as

$$\Delta_{\text{down}} = \Delta_{\text{up}} \frac{\text{BLER}_{\text{target}}}{1 - \text{BLER}_{\text{target}}}. \quad (3.9)$$

for a given BLER target and  $\Delta_{\text{up}}$ .

An ILLA [77] selects an appropriate MCS for each scheduled user. The procedure is the following. First, the exponential effective SINR [17, 28] is calculated for every supported MCS based on corrected CQIs. It is later used to evaluate the expected instantaneous throughput. Finally, the modulation and coding scheme that maximizes the expected throughput is chosen for the next transmission.

### 3.3.5 Hybrid-ARQ

Automatic Repeat Request (ARQ) uses an error-decoding code, such as Cyclic Redundancy Check, to identify the erroneous transmission and to request the retransmission if needed. Hybrid ARQ is a combination of ARQ and forward error correcting code. Forward error correcting is used to correct a subset of all errors. The uncorrectable errors are detected by ARQ process and retransmission is requested. The Cyclic Redundancy Check is used for error detection and Turbo codes are used for error correction [23]. The HARQ strategy is applied on the physical layer in order to reduce the retransmission delays.

The HARQ process distinguishes two categories based on timing for

retransmission. In the asynchronous HARQ the retransmission can be scheduled in any time after received negative acknowledgment. In the synchronous HARQ the retransmissions are scheduled at fixed time intervals.

The HARQ strategy uses stop-and-wait mode, where several parallel stop-and-wait channels are organized. In each channel independent HARQ process takes place. Since the retransmission can be scheduled only after a certain delay, stop-and-wait mode allows to perform the retransmission for other HARQ processes for the same user during the delay time period.

The HARQ with soft combining [23] combines the erroneously received packet with the retransmitted packet. As a result, the combined packet is more reliable and the stored information is efficiently utilized. The retransmitted packet contains the same information bits, but the coded data can differ. The HARQ with Chase Combining uses the same code data, and the identical data are retransmitted. The same modulation and coding scheme is utilized for the transmission and retransmission.

The HARQ gain modeling presented in [34] is used to define combined effective SINR after  $r$  retransmissions by the following recursion

$$(\gamma_n^{\text{eff}})_{\hat{\mathcal{R}}} = \epsilon^{\hat{\mathcal{R}}-1} \nu(\text{ECR}, l)_{\hat{\mathcal{R}}} \sum_{\rho=1}^{\hat{\mathcal{R}}} (\gamma_n^{\text{eff}})_{\rho}, \quad (3.10)$$

where parameter  $\epsilon$  represents chase combining efficiency,  $\nu(\text{ECR}, l)_{\hat{\mathcal{R}}}$  is incremental redundancy gain over chase combining for  $\hat{\mathcal{R}}$  transmission ( $\nu(\text{ECR}, l)_{\hat{\mathcal{R}}} = 1$  in case of chase combining),  $\gamma_n^{\text{eff}}$  is the effective SINR calculated via the exponential effective SINR mapping [17, 28] for  $n$ -th spatial data stream.

### 3.3.6 Handover

In 3GPP LTE network the handover [12, 46, 59] is controlled by the network. Base station makes a decision about the handover and the assigned cell based on measurements made by mobile terminal. Mobile terminal processes the channel measurements from the serving cell and all neighboring cells in order to average out fast-fading fluctuations and estimation errors. The Reference Signal Received Power (RSRP), Received Signal Strength Indicator (RSSI) and Reference Signal Received Quality (RSRQ) measurements are made using cell-specific downlink reference symbols [59].

RSRP is measured for a specific cell as an averaged received power ob-

served by mobile terminal over all reference symbols within the measurement bandwidth. RSSI is the total received wideband power observed by mobile terminal from all the sources from all cells in the network. RSRQ is the ratio between RSRP and RSSI measurements.

Mobile terminal makes the RSRP and RSSI measurements with predefined measurement interval and collects them. The collected measurements are averaged over specific time period. The RSRP measurement is calculated from the averaged RSRP and RSSI values. Mobile terminal reports all the measurements to the base station in event-triggered manner.

The hard handover procedure is performed to relocate mobile terminal from one base station to the other. Hard handover procedure is fast and beneficial in the distributed networks, where mobility control moves to the base stations.

The hard handover is triggered by the base station based on reported RSRQ measurement provided by mobile terminal. If the measurement is below parameterized threshold (handover margin), then the handover is triggered. The base station negotiates the handover with the user and target base station. During handover process user can not be scheduled. After successful connection to target base station, both scheduling and HARQ processes can be continued normally [59].

### 3.4 Simulation scenario

The 3GPP claims in [72] that the simulation scenarios aiming various research groups have to be agreed for comparison of the simulation results without real implementation of the proposed algorithms.

In this thesis fully dynamic time-driven simulator has been utilized to study the effect of proposed algorithms on final system performance. The full set of agreed parameters for 3GPP LTE network simulations can be found in [3, 72].

The simulated macro cellular network with the hexagonal grid cell layout with parameterized Inter-Site Distance (ISD) is standardized as simulation scenario in [69]. The basic layout for macro deployment scenario shown in Figure 3.4(b) is simulated in Publication I. More sophisticated three-tier macrocell scenario shown in Figure 3.4(a) with wrap around is simulated in Publication II, Publication III, Publication IV, Publication V,

**Table 3.2.** 3GPP simulation cases.

<b>Simulation Case</b>	<b>CF (GHz)</b>	<b>ISD (m)</b>	<b>BW (MHz)</b>	<b>Ploss (dB)</b>	<b>Speed (kmph)</b>
1	2.0	500	10	20	3
2	2.0	500	10	10	30
3	2.0	1732	10	20	3
4	0.9	1000	1.25	10	3

Publication VI in order to reduce edge effects that can distort the results. The mobile stations are uniformly distributed over the simulation area. Low (3kmph), medium (30 kmph) and high (120 kmph) mobility scenarios are analyzed. Four standardized macro deployment scenarios called 3GPP Cases 1–4 [3] with specified BandWidth (BW), Central Frequency (CF), Inter–Site Distance (ISD), Penetration Loss (Ploss) and Speed of mobile terminal (Speed) are shown in Table 3.2.

In the simulations, complex fast fading samples from the used tapped delay line model is generated where each tap fades according to the Jakes model [50]. Lognormally distributed samples with parameterized standard deviation are added to the signal to simulate the slow fading samples. The spatial autoregressive [41] and base station correlation [64] models are used to produce the correlated slow fading samples. The Okamura-Hata model [44, 70] is used for distance dependent pathloss.

In the simulations, infinite buffer traffic model is used for high load scenario. Inner loop and outer loop link adaptation with QPSK, 16QAM and 64QAM modulation schemes and various code rates is utilized for fast adaptation to changing channel conditions. The maximum throughput, proportional fair and round robin packet scheduling algorithms are used in time and frequency domain with "Per-Resource" mode prioritizing re-transmissions. HARQ with asynchronized Chase Combining is used to correct the packet transmission. Network controlled hard handovers with averaging over the sliding window and predefined handover margin are modeled.

The most important simulation parameters that are used to produce the simulation results in the publications of author are summarized in Table 3.4.



### 3.5 Performance evaluation

The performance evaluation can be done from the end-user and the system operator perspective as shown in [23]. The subscribers are willing to get the best quality, such as user throughput, network latency and setup time, where the operators prefer to get the highest profit, for example in terms of number of subscribers. Due to the limited resources there is always a trade-off between the operator profit and the end-user profit. For the 3GPP LTE performance evaluation both the end-user and the system operator evaluation measures should be estimated.

The 3GPP in [4] has defined a set of performance targets and requirements for the 3GPP LTE development with the following key elements. Here, the reference system used for comparison is 3G UMTS HSPA Release 6 with simple receiver and 1x2 SIMO DL and 1x1 SISO UL transmission [46].

1. Peak data rates requirements are 100 Mbps for downlink (2x2 MIMO) and 50 Mbps for uplink (1x2 SIMO) transmission in 20 MHz channel.
2. Mean user throughput should be 3 and 2 times higher for downlink and uplink, respectively, compared to HSPA Rel.6.
3. Cell-edge throughput should be 2 times higher for both downlink and uplink compared to HSPA Rel.6.
4. Spectral efficiency should be 3 and 2 times higher for downlink and uplink, respectively, compared to HSPA Rel.6.
5. Improved latency is required to be below 10 ms from a mobile terminal to a server.
6. Spectrum flexibility from 1.4 till 20 MHz bandwidth allocation is required.
7. Optimized performance for low speed up to 15 kmph, high performance at speed up to 120 kmph, maintain link at speed up to 350 kmph are required.
8. Coverage with full performance up to 5 km, slight degradation of per-

formance from 5 to 30 km, possible coverage up to 100 km are required.

9. Reduced cost is desired for operators and subscribers.

The HSPA Rel.6 performance evaluation in 3GPP Case 1 scenario is summarized in Table 3.3.

The requirements for the performance specify the performance measures. The key performance measures from system point of view are capacity and spectral efficiency. The key performance measures from user point of view are mean user throughput and cell-edge user throughput. The simulation results of performance evaluation are discussed later in section 5.3.

The spectral efficiency as one of the key indicator of performance can be defined as [23]

$$S = \frac{N_{\text{bits}}}{\text{BW}\Delta T N_{\text{cells}}[\text{bits/s/Hz/cell}]}, \quad (3.11)$$

where  $N_{\text{bits}}$  is the number of successfully received bits, BW is an utilized bandwidth,  $\Delta T$  is the simulation time duration,  $N_{\text{cells}}$  is number of cells in the network.

Figure 3.5 illustrates the spectral efficiency (3.11) for 3GPP LTE down-link network evaluated by fully dynamic SLS ("NOKIA NRC" in Figure 3.5). This simulator has been used to provide the simulation results for the system performance evaluation in the publications of author. Figure 3.5 also presents the performance results provided by Nokia semi-static SLS ("NOKIA" in Figure 3.5) and other companies. All the results are very well in line. The differences can be explained mainly by different parameter settings as well as dynamic or semi-static nature of the simulators.

**Table 3.3.** The HSPA Rel.6 performance evaluation in 3GPP Case 1.

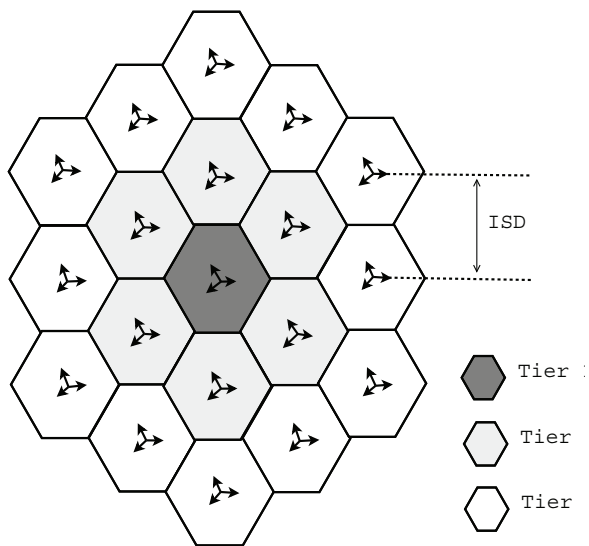
Direction	Spectral Efficiency	Mean User Throughput	Cell-Edge User Throughput
1x2 SIMO DL [30]	0.53 bps/Hz/cell	0.05 bps/Hz	0.02 bps/Hz
1x1 SISO UL [68]	0.332 bps/Hz/cell	0.033 bps/Hz	0.009 bps/Hz

### 3.6 Discussion

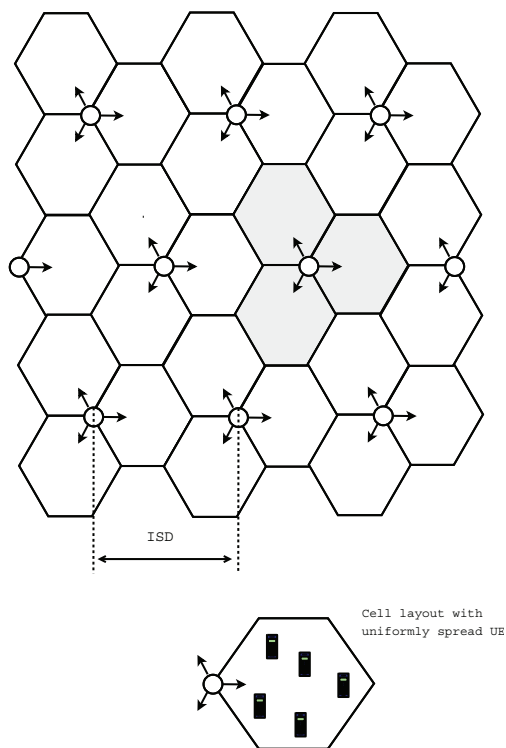
In this chapter the simulation methodologies on the system level are discussed. Various types of system level simulators has been analyzed and compared. The main differences among them are summarized in Table 3.1.

In general, for the system performance evaluation different statistical approaches, system dynamic effects and simplicity of the implementation of system functionality should be considered in order to get the results at different computational costs. The static simulator is easy to implement and fast in result production, but it tends to overestimate the system performance. The dynamic simulator is much more complex, but provides more accurate performance results and allows to measure the impact of dynamic effects on system performance. Therefore, for the network planning and optimization purposes both static and dynamic tools are needed in order to obtain an efficient network model at reasonable computational cost.

In this chapter the advanced RRM functionality including packet scheduling, link adaptation, CQI manager, HARQ process, handover functionality are explained in detail. The main simulation parameters for RRM algorithms used in the publications of author are presented in Table 3.4. Verification of performance metrics, simulation assumptions and simulation scenarios is crucial in order to compare the simulation results from different simulators. The obtained performance results show that the simulations on agreed parameters give very similar results to those produced by other research groups.



(a) Three tier macrocell scenario with 19 sites of 3 sectors, to- tally 57 cells.



(b) Macrocell scenario with 9 sites of 3 sectors, totally 27 cells.

**Figure 3.4.** Simulation layout for macro deployment scenario, where base station has antenna with sector center direction.

**Table 3.4.** Simulation parameters.

<b>Parameter description</b>	<b>Parameter value</b>
Scenario	macrocell scenario synchronized downlink
Bandwidth	20MHz 10MHz Publication II, Publication VI
Carrier Frequency	5GHz Publication I, 2GHz
Simulation time step	subframe = 1 ms (RRM, scheduling), OFDM symbol = 66.7 $\mu$ s, OFDM symbol = 22 $\mu$ s Publication I
Distance-dependent pathloss	$128.1 + 37.6 \log_{10}(\text{distance})$
shadowing standard deviation	6 dB Publication I, 8 dB
shadowing correlation (sites/sectors)	0.5 / 1.0
BS power	43 dBm Publication I, 46 dBm
noise power at MT	-94.0 dBm Publication I, -123.2 dBm
UE velocity	3, 30 and 120 km/h
Traffic model	Infinite Buffer
Link Adaptation	Inner loop and outer loop LA
MCS	QPSK 1/3, 1/2, 2/3 16QAM 1/2,2/3,4/5 64QAM 1/2,2/3,4/5
OLLA	BLER target = 0.2 $\Delta_{\text{up}} = 0.5$
CQIs	5 ms measurement period 1 dB error variance 1 dB quantization step 2 ms reporting delay 2 resource blocks per CQI
Packet scheduling	TD: MT, PF, RR FD: MT, PF, RR 5 maximum scheduled users "Per-Resource" mode
Hybrid ARQ	Asynchronous Chase Combining 6 stop-and-wait processes max 3 retransmissions
ARQ	Off
Power Control	Off
Handovers	hard handovers 50ms measurement interval 200 ms sliding window 200ms reporting interval 3 dB handover margin

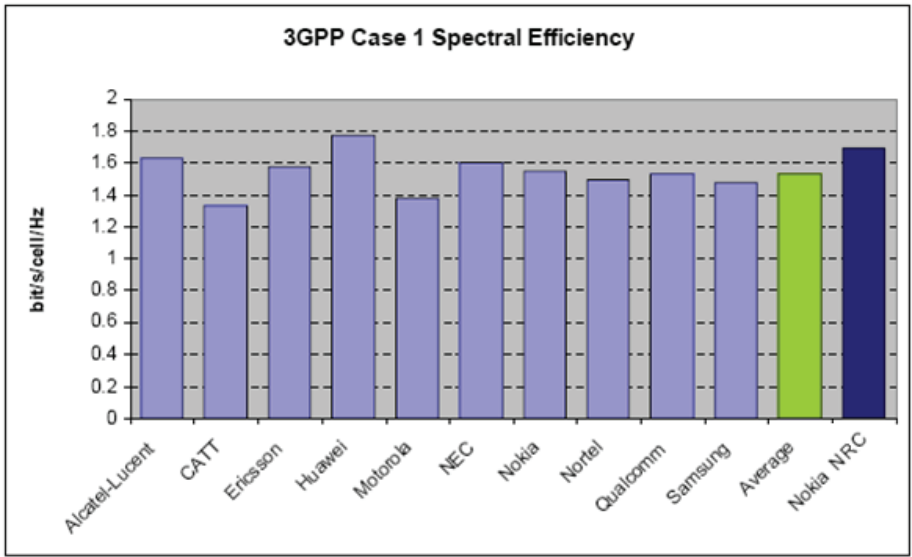


**Figure 3.5.** Benchmarking LTE spectral efficiency compared with different references.

## 4. Link-to-System Interface

The task of Link-to-System interface is to provide a simple but accurate link performance prediction model. L2S interface simplifies the simulations needed to evaluate the performance of future wireless broadband networks. It substitutes the complex link level simulations of performance evaluation of all radio links between base stations and mobile terminals in the network into a simple link error prediction model. The target of such prediction model is to transfer the accuracy of the actual performance of the receiver from the link level to the system level.

Traditionally, the link performance model [19,61,104] is realized through a set of Look-up Tables (LuT) obtained from the link level simulations. These mapping tables provide the interface between link and system level simulations and give tabulated coded BLER as a function of SNR. For the single carrier system the BLER as a function of an average SNR for a specific channel has been used to characterize an average system performance. Such L2S interface approach is reasonable for a system, where packet duration is much longer than the channel coherence time and every transmission can be characterized by similar channel statistics [95]. But for the multi-carrier system with relatively short packet duration, the predicted performance from the averaged curves may be not accurate enough as shown in [60] and in Figure 4.1. In multi-carrier system frequency selectivity allows the same average SINR to yield different performance in terms of BLERs. Moreover, the performance enhancement of future wireless system can be achieved by means of the channel adaptive transmission techniques such as channel-dependent scheduling and fast link adaptation. That means, that instantaneous channel state and interference conditions should be taken into account for the link error prediction model. Additionally, generic L2S interface is desired to be simple, independent on the channel type and Doppler spread in order to be

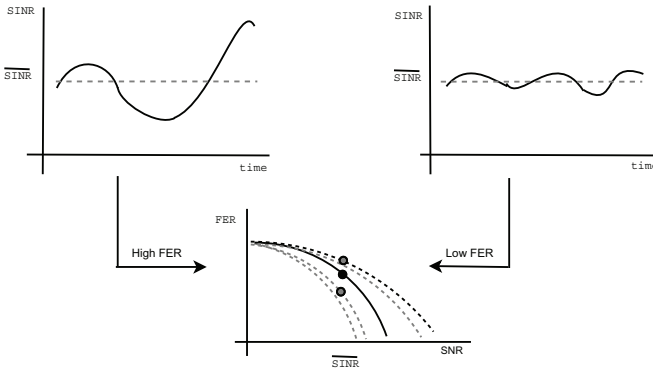


**Figure 4.1.** Example of different FER probability with the same mean SINR value. High mobile speed and high interference variance provide highly-varying SINR. Low mobile speed and fast power control provide less-varying SINR. Both examples give the same mean SINR value. But the higher variance of SINR yields higher FER probability with the same mean SINR value [60].

applicable in a real system and do not require exhaustive simulation campaigns [27, 95]. Revising L2S interface methods for single carrier system, utilizing their potentials and improving their drawbacks, the generic L2S interface for multi-carrier system has been created.

The generic L2S interface is a quality model that facilitates accurate estimation of the performance of each link knowing the block length, physical transmission mode, resource allocation, propagation conditions, intercell interference, etc. A generic L2S interface determines the block error rate of a link based on instantaneous channel state, independently of channel type or user speed. The generic L2S interface compresses the set of all resource quality measures into one effective SINR value in order to reduce impracticable multi-dimensional mapping into one-dimensional mapping.

In this chapter L2S interface methods for single carrier systems are discussed in section 4.1. The generic L2S interface for multi-carrier systems is presented in section 4.2. The realization of generic L2S interface through the effective SINR mapping is presented in section 4.3. A comparison of different effective SINR approaches is provided in section 4.4. Focusing on exponential effective SINR, the distribution of effective SINR is considered in section 4.5.



#### 4.1 Traditional L2S interface

Several L2S interface methods are proposed and used for single carrier systems such as GSM, EDGE, 3G CDMA-based system, in order to quantify the link quality on the system level. The most widely used models are described below and their pros and cons are discussed.

The Average Value Interface (AVI) [61, 104] is based on the local mean of SNR values at all receivers in the system per simulation time step. The mean SNR is later mapped to BLER value using look-up tables.

$$\gamma_{\text{AVI}} = \frac{1}{K} \sum_{k=1}^K \gamma_k \quad (4.1)$$

$$\text{BLER} = f_{\text{LuT}}(\gamma_{\text{AVI}}) \quad (4.2)$$

This approach does not take into account time-varying nature of the channel quality, since the SNR calculation is based on propagation model that includes only pathloss and shadow fading. Thus, it is applicable only in AWGN or slow fading channel environment. However, same average SNR can lead to different link performance, i.e. the channel with less variation shows better performance than the channel with more variation [94].

The Actual Value Interface (AcVI) [43, 71, 105] has been introduced in order to capture fast changes in the channel quality. In this model the BLER value as a link quality indicator is estimated in two steps. Each observed SINR value is mapped to bit error rate value via look-up tables, then the mean value and the standard deviation of bit error rates within a block are used for mapping to BLER via look-up tables.

$$\text{BER}_k = f_{\text{LuT}}(\gamma_k), \quad k = 1 : K \quad (4.3)$$

$$\mu_{\text{BER}} = \frac{1}{K} \sum_{k=1}^K \text{BER}_k \quad (4.4)$$

$$\sigma_{\text{BER}}^2 = \frac{1}{K} \sum_{k=1}^K (\text{BER}_k - \mu_{\text{BER}})^2 \quad (4.5)$$

$$\text{BLER} = f_{\text{LuT}}(\mu_{\text{BER}}, \sigma_{\text{BER}}^2) \quad (4.6)$$

The disadvantages of the model are the following. The number of look-up tables is very large, since one table is required per modulation, per data size (burst or frame), per channel model, per discrete speed value, per service. Also the method requires averaging over multiple frames to provide accurate results.

The Actual Value Interface does not take into account the influence of each multipath component. Therefore, other L2S interface is designed for

CDMA-based technology in order to evaluate the receiver performance where signal power distribution in each path is important [74, 79, 87]. The model consists of two-dimensional mapping from an orthogonality factor and SINR value to bit error rate. The orthogonality factor is an indicator how much the orthogonality among the spreading codes is lost due to multipath dispersion. The averaged bit error rate within a block is later mapped to BLER as follows

$$\text{BER}_k = f_{\text{LuT}}(\gamma_k, \text{OF}), \quad k = 1 : K \quad (4.7)$$

$$\mu_{\text{BER}} = \frac{1}{K} \sum_{k=1}^K \text{BER}_k \quad (4.8)$$

$$\text{BLER} = f_{\text{LuT}}(\mu_{\text{BER}}). \quad (4.9)$$

Extensive link level simulations are required to construct the look-up tables for the broad but dense range of different SNR values and orthogonal factors. Moreover, significant averaging of bit error rates within a block is required for accurate prediction of the link quality.

In order to reduce the number of look-up tables, a Quasi-Static L2S interface methodology (QS) is proposed for CDMA-based systems in [6, 82]. In the quasi-static approach the block error rate is obtained by using the adjusted block SNR in the corresponding static AWGN reference curve for QPSK modulation and 1/5 coding rate. The SNR in the block is calculated by averaging of the instantaneous received SNR of each information bit within a block. Due to the difference between actual link performance and reference AWGN performance, the SNR is adjusted using several penalty factors  $P_i$ . The penalty factors take into account the degradation generated by high coding rate, high modulation order or high mobility.

$$\gamma_k = \gamma_k - \sum_i P_i, \quad k = 1 : K \quad (4.10)$$

$$\gamma_{\text{QS}} = 10 \log_{10} \left( \frac{1}{K} \sum_{k=1}^K \gamma_k \right) \quad (4.11)$$

$$\text{BLER} = f_{\text{LuT}}(\gamma_{\text{QS}}) \quad (4.12)$$

The method requires a table of all possible penalty factors to be pre-calculated for different SNR values. The quasi-static fading model requires the variations of the channel to be small over a codeword. Hence, it is not applicable in the frequency domain for broadband system.

The L2S interface based on modified Shannon's channel capacity [13, 81, 93] is investigated as an alternative approach to penalty-based quasi-static L2S interface. An effective quality measure of the link is calculated

per block as an average of modified channel capacities for each SNR value. The obtained quality measure either can be used to estimate the block error rate from corresponding AWGN reference curve per data size (block or frame) and code rate [81, 93] or can be converted to a modulation and coding scheme needed for link adaptation [13] using the following equations:

$$C_k = \log(1 + \eta\gamma_k), \quad k = 1 : K \quad (4.13)$$

$$\mu_C = \frac{1}{K} \sum_{k=1}^K C_k, \quad (4.14)$$

$$\gamma_{\text{eff}} = \frac{2^{\mu_C} - 1}{\eta}, \quad (4.15)$$

$$\text{BLER} = f_{\text{LuT, AWGN}}(\gamma_{\text{eff}}), \quad (4.16)$$

where  $\eta$  is a correction factor included to account for practical performance degradation from Shannon's capacity limit.

This approach needs a calibration using a large number of different channel types in order to define the correction factor for the modified channel capacity metric. However, the L2S interface based on modified Shannon's channel capacity is considered to be promising in [81, 93], since it can handle the channel variations in the frequency domain. It is later taken into account for the effective SINR mapping.

## 4.2 Generic L2S interface

The progress of wireless communication networks imposes requirements on the link performance model, since OFDM-based transmission technology is the main access method for beyond-third-generation mobile broadband system. Consequently, the following requirements for the L2S interface model should be fulfilled.

- L2S interface should capture fast channel variations in the frequency domain.
- L2S interface should be independent of the channel type.
- L2S interface should be independent of the Doppler spread.
- L2S interface should determine an instantaneous BLER based on instantaneous fading profile.

Different L2S approaches for multi-carrier systems are discussed in [7,

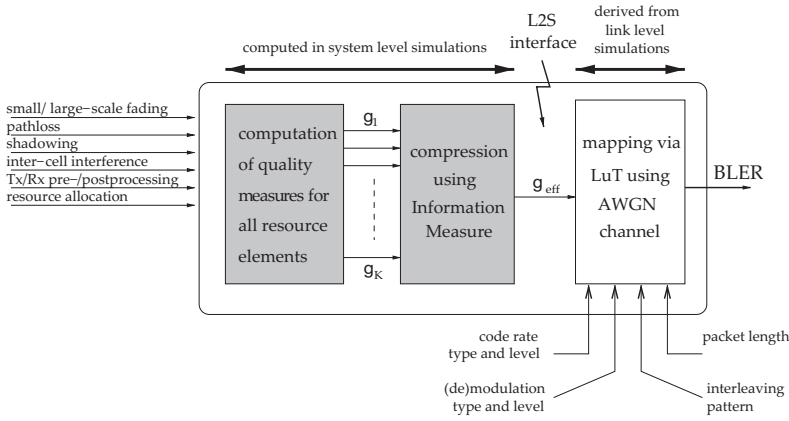


**Figure 4.2.** L2S interface model for the system level performance evaluation.

26, 28, 29, 53, 66, 67, 95]. A generic L2S interface model, that satisfies the requirements for the link performance model and generalizes the discussed approaches, is introduced in [17].

Figure 4.2 presents the generic L2S interface model for the system level performance evaluation. At each step of system level simulator the users are scheduled according to specific scheduler metric and the resources are allocated among the users. The individual instantaneous channels including small- and large-scale fading, path loss and interference are modeled. The set of quality measures, such as post-processed SINR values, are derived for all resource elements in frequency and in time. For an OFDM system the data packet of the user may occupy several OFDM symbols in time and several OFDM sub-carriers in frequency. Hence, the number of time and frequency resource elements to be measured is too large and the compression from instantaneous channel state to the smaller number of quality measures is required. Typically, one or two scalar quantities that characterize the channel state are desired to predict the final block error rate. The BLER can be found through look-up table from the pre-calculated BLER performance of AWGN channel corresponding to a given modulation and coding scheme combination. The AWGN channel performance can be obtained either from the link level simulations or through theoretical analysis. Finally, successful coded block transmission is determined based on random experiment with BLER probability of error.

This model can be adapted to a MIMO context. In multi-stream transmission independent error prediction using presented L2S interface model is applied for each stream. The benefit of separate stream performance evaluation is in independent link adaptation (MCS selection) and HARQ

processing for each stream.

### 4.3 Effective SINR mapping

For the sake of simplicity an one-dimensional mapping is considered to be the most promising for generic L2S interface given in section 4.2. The Effective SINR Mapping (ESM) approach is proposed in [26, 28]. The ESM maps the instantaneous channel state characterized by  $K$  quality measures of time/frequency/space resource elements denoted by  $\{\gamma_1, \gamma_2, \dots, \gamma_K\}$  into an instantaneous effective quality measure  $\gamma_{\text{eff}}$ . Afterwards, the effective quality measure is mapped to the performance metric, such as BLER, in a single-state channel via AWGN performance curves. The objective of the ESM approach is to provide the following approximation:

$$\text{BLEP}_{\text{AWGN}}(\gamma_{\text{eff}}) \approx \text{BLEP}(\{\gamma_1, \gamma_2, \dots, \gamma_K\}), \quad (4.17)$$

meaning that for any channel type the actual block error probability for instantaneous channel state is equivalent to the AWGN Block Error Probability (BLEP) corresponding to the effective quality measure.

Several methods for ESM mapping function are proposed in [7, 8, 27, 28, 53]. The general principle of mapping is formulated in [17]. For a given instantaneous channel state with  $K$  different quality measures of resource elements denoted by  $\{\gamma_1, \gamma_2, \dots, \gamma_K\}$ , the effective quality measure  $\gamma_{\text{eff}}$  can be defined as

$$\gamma_{\text{eff}} = \alpha_1 \mathcal{I}^{-1} \left( \frac{1}{K} \sum_{k=1}^K \mathcal{I} \left( \frac{\gamma_k}{\alpha_2} \right) \right), \quad (4.18)$$

where  $\mathcal{I}$  is specified information measure function [27] and  $\mathcal{I}^{-1}$  is the inverse function. Usually  $\{\gamma_1, \gamma_2, \dots, \gamma_K\}$  are the received post-processed SINR values within a coded transport block. The scalars  $\alpha_1$  and  $\alpha_2$  are adjusted through the ESM principle given by equation (4.17) for a given MCS by minimizing the square error between the estimated BLER,  $\text{BLER}_c(\gamma_{\text{eff}}, \alpha_1, \alpha_2)$ , and simulated BLER,  $\text{BLER}_c$ , over  $N_c$  link level simulations for the same MCS as

$$(\alpha_1, \alpha_2) = \underset{\alpha_1, \alpha_2}{\text{argmin}} \sum_{c=1}^{N_c} |\text{BLER}_c(\gamma_{\text{eff}}, \alpha_1, \alpha_2) - \text{BLER}_c|^2. \quad (4.19)$$

Minimization can be done in logarithmic domain in order to get lower squared error in lower BLER regime.

The purpose of information measure function is to characterize the channel capacity with perfect channel state information as shown in [27]

$$\mathcal{I}(\gamma_{\text{eff}}) = \begin{cases} \int \mathcal{I}(\gamma) f_{\Gamma}(\gamma) d\gamma, & \text{if } \gamma \text{ continuous} \\ \sum_{k=1}^K \mathcal{I}(\gamma_k) \mathbf{p}_k, & \text{if } \gamma_k \text{ discrete} \end{cases} \quad (4.20)$$

where  $\gamma_{\text{eff}}$  is the effective quality measure,  $f_{\Gamma}(\gamma)$  is the pdf for continuous-valued resource quality measure  $\gamma$ ,  $\mathbf{p}_k$  is the probability mass function for discrete-valued resource quality measure  $\gamma_k$ .

The commonly known information measures studied in [7, 8, 27, 28, 53] are listed below along with the effective SINR fitted into general form given in equation (4.18).

1. The capacity effective SINR mapping [8],  $\gamma_{\text{eff}}$ , is defined as

$$\gamma_{\text{eff}} = \beta \left( 2^{\frac{1}{K} \sum_{k=1}^K \log_2(1 + \frac{\gamma_k}{\beta})} - 1 \right). \quad (4.21)$$

It is based on the capacity

$$\mathcal{I}(\gamma) = \log_2(1 + \gamma) \quad (4.22)$$

with adjustment coefficient  $\beta = \alpha_1 = \alpha_2$  in (4.18).

2. Logarithmic effective SINR mapping [53] is defined as

$$\gamma_{\text{eff}} = 10^{-\beta \sigma^2 (\log_{10}(\gamma_k))} 10^{\frac{1}{K} \sum_{k=1}^K \log_{10}(\gamma_k)}. \quad (4.23)$$

It is based on logarithm function that represents SINR value in dB scale

$$\mathcal{I}(\gamma) = \log_{10}(\gamma) \quad (4.24)$$

with different adjustment coefficients  $\alpha_1 = 10^{-\beta \sigma^2 \log_{10}(\gamma_k)}$  and  $\alpha_2 = 1$  in (4.18). Here,  $\sigma^2$  denotes the variance of SINR values in logarithmic scale.

3. Cutoff rate effective SINR mapping [27] is defined as

$$\gamma_{\text{eff}} = -2\beta \ln \left( 2^{\frac{1}{K} \sum_{k=1}^K \log_2(1 + e^{-\frac{\gamma_k}{2\beta}})} - 1 \right). \quad (4.25)$$

It is based on the cutoff rate, that is for BPSK modulation is given by

$$\mathcal{I}(\gamma) = 1 - \log_2(1 + e^{-\frac{\gamma}{2}}), \quad (4.26)$$

and adjustment coefficient  $\beta = \alpha_1 = \alpha_2$  in equation (4.18).

4. Linear SINR mapping [27] as an adaptation of AVI described in section 4.1 to the generic L2S interface given in equation (4.18) is defined as an average

$$\gamma_{\text{eff}} = \frac{1}{K} \sum_{k=1}^K \gamma_k. \quad (4.27)$$

It based on the quality measure itself, i.e. linear SINR value, as

$$\mathcal{I}(\gamma) = \gamma. \quad (4.28)$$

The most potential and significant mapping functions of form of equation (4.18) are exponential and mutual information-based effective SINR mapping, EESM and MI-ESM respectively. EESM and MI-ESM are discussed and adopted in 3GPP feasibility study on OFDM [65] and is applicable in 3GPP LTE, 802.11 WLAN and 802.16 WiMAX.

### *EESM*

The objective of the EESM [28] is to find an effective quality measure that brings the same Chernoff bounded error probability as transmission over  $K$  AWGN channels.

Let consider an example. The error probability  $P_e$  for BPSK transmission over AWGN channel can be upper bounded by Chernoff bound in high SINR regime as follows

$$P_e(\gamma) = Q(\sqrt{2\gamma}) \leq e^{-\gamma} \quad (4.29)$$

$$Q(x) = \frac{1}{\sqrt{2\pi}} \int_x^{\infty} e^{-\frac{u^2}{2}} du. \quad (4.30)$$

Combining the Union bound with the Chernoff bound, the block error probability  $\mathcal{P}_e$  for the transmission of the block of  $K$  symbols over  $K$  AWGN channels can be evaluated as follows

$$\mathcal{P}_e \leq \sum_{k=1}^K e^{-\gamma_k}. \quad (4.31)$$

The effective quality measure,  $\gamma_{\text{eff}}$ , is defined using the combined Union-Chernoff bound of block error probability  $\mathcal{P}_e$  as

$$\mathcal{P}_{e, \text{Union-Chernoff Bound}}(\{\gamma_1, \gamma_2, \dots, \gamma_K\}) = \mathcal{P}_{e, \text{Union-Chernoff Bound}}(\gamma_{\text{eff}}), \quad (4.32)$$

and, consequently,

$$\sum_{k=1}^K e^{-\gamma_k} = \sum_{k=1}^K e^{-\gamma_{\text{eff}}} \Rightarrow \gamma_{\text{eff}} = -\ln \left( \frac{1}{K} \sum_{k=1}^K e^{-\gamma_k} \right). \quad (4.33)$$

The derivations of  $\gamma_{\text{eff}}$  using combined Union-Chernoff bound technique for higher order modulation schemes are presented in [28]. To adjust the

model to different modulation and coding schemes, a scaling parameter  $\beta$  is incorporated into the mapping. The EESM may then be defined as

$$\gamma_{\text{eff}} = -\beta \ln \left( \frac{1}{K} \sum_{k=1}^K e^{-\frac{\gamma_k}{\beta}} \right). \quad (4.34)$$

The generalized expression for the exponential effective SINR mapping (4.34) shows that the information measure function is exponential

$$\mathcal{I}(\gamma) = A - B e^{-\frac{\gamma}{\beta}}, \forall A, B \in \mathbb{R} \quad (4.35)$$

and the EESM fits into the general L2S interface given in equation (4.18). The adjustment of the scaling parameter  $\beta$  for each MCS is done on the link level providing the best matching according to equation (4.19).

### MI-ESM

The Mutual Information SINR mapping [27] is based on a mutual information based metric. The modulation constrained capacity represents the mutual information of a symbol channel [90], i.e., channel with input symbols from a complex set. The bit-interleaved coded modulation capacity is considered as the mutual information measure function [11]. It is given by [18]

$$\mathcal{I}_{m_k}(\theta) = m_k - E_Y \left( \frac{1}{2^{m_k}} \sum_{i=1}^{m_k} \sum_{b=0}^1 \sum_{z \in \Gamma_b^i} \log_2 \frac{\sum_{\hat{\theta} \in \Gamma} e^{-|Y - \sqrt{\theta}(\hat{\theta} - z)|^2}}{\sum_{\hat{\theta} \in \Gamma_b^i} e^{-|Y - \sqrt{\theta}(\hat{\theta} - z)|^2}} \right), \quad (4.36)$$

where  $m_k$  is the number of bits per symbol  $k$ ,  $\Gamma$  is the set of  $2^{m_k}$  symbols,  $\Gamma_b^i$  is the set of symbols for which bit  $i$  equals to  $b$ ,  $Y$  is a zero mean unit variance complex Gaussian variable. In general, expectation in equation (4.36) can not be calculated in a closed form and the Monte Carlo simulations are used instead. At the system level simulations pre-calculated tables for bit-interleaved coded modulation capacity are utilized. The bit-interleaved coded modulation capacity for different modulation schemes is illustrated in Figure 4.3.

The effective SINR value,  $\gamma_{\text{eff}}$ , is obtained using general L2S interface shown in equation (4.18) with adjacent parameter  $\beta = \alpha_1 = \alpha_2$  as follows

$$\gamma_{\text{eff}} = -\beta \mathcal{I}_{m_{\text{ref}}} \left( \frac{1}{K} \sum_{k=1}^K \mathcal{I}_{m_k} \left( \frac{\gamma_k}{\beta} \right) \right), \quad (4.37)$$

where  $m_{\text{ref}}$  is an average number of transmitted bits per data symbol,  $m_{\text{ref}} = \frac{1}{K} \sum_{k=1}^K m_k$ .

Another information measure function is used in [7]. It is also based on the constrained capacity

$$\mathcal{I}(\theta) = C_M(\gamma) = \int_C p_N(n) \log_2(p_N(n)) dn - \int_C p_Y(y) \log_2(p_Y(y)) dy, \quad (4.38)$$



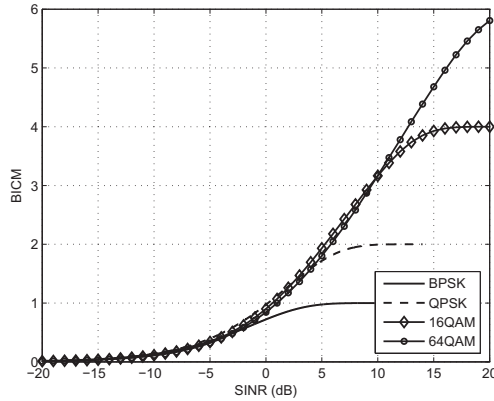


**Figure 4.3.** The bit-interleaved coded modulation capacity (BICM) for BPSK, QPSK, 16QAM and 64QAM modulation.

where  $p_N(n)$  is the pdf of random variable  $N$ , usually  $N \sim \mathcal{CN}(0, 1)$ ,  $p_Y(y)$  is the pdf random variable  $Y = X + N$ , where power of random variable  $X$  is  $E\{|X|^2\} = \gamma$ ,  $M$  is the specified modulation. So, the capacity is constrained by given modulation scheme. The adjustment coefficients are equal to one in this model,  $\beta = \alpha_1 = \alpha_2 = 1$ . The resulting effective SINR  $\gamma_{\text{eff}}$  is given by

$$\gamma_{\text{eff}} = C_M^{-1} \left( \frac{1}{K} \sum_{k=1}^K C_M(\gamma_k) \right). \quad (4.39)$$

#### 4.3.1 Calibration of the scaling parameter $\beta$

Both EESM and MI-ESM models require the scaling parameter  $\beta$  in order to adjust the effective SINR to a specific modulation and coding rate as shown in [17]. It has been observed that in the AWGN channel for BPSK transmission  $\beta$  has no impact to the effective link quality measure, i.e.  $\beta = 1$ . So, the effective SINR is equal to all measured instantaneous SINR values, i.e.  $\gamma_{\text{eff}} = \gamma_k \forall k = 1 : K$ . Hence, the AWGN performance curve fits perfectly for the reference mapping.

The calibration of  $\beta$  scaling parameter for a given MCS is done by means of the link level simulations according to principle given in equation (4.19). On the link level  $N_c$  channel realizations are made for several channel models. For each channel realization, that is characterized by a set of post-processed SINRs,  $\{\gamma_1^c, \gamma_2^c, \dots, \gamma_K^c\}$ , BLER value,  $\text{BLER}_c$ , is obtained from the link level simulations through averaging. Another BLER value,  $\text{BLER}_c(\gamma_{\text{eff},c}, \beta)$  for the candidate value of  $\beta$  is estimated from AWGN

reference curve for given MCS based on effective SINR value,  $\gamma_{\text{eff},c} = \beta \mathcal{I}^{-1} \left( \frac{1}{K} \sum_{k=1}^K \mathcal{I} \left( \frac{\gamma_k}{\beta} \right) \right)$ . Minimizing the squared difference between the simulated BLER,  $\text{BLER}_c$ , and estimated BLER,  $\text{BLER}_c(\gamma_{\text{eff},c}, \beta)$ ,  $\beta$  value is determined as

$$\beta = \arg \min_{\beta} \sum_{c=1}^{N_c} (\text{BLER}_c - \text{BLER}_c(\gamma_{\text{eff},c}, \beta))^2. \quad (4.40)$$

The enhanced version of calibration procedure is proposed in [45], where a weighted squared difference is minimized for the adjustment of scaling parameter. The properly chosen weights in low and high BLER regions provide higher accuracy of the adjustment of  $\beta$  coefficient. Consequently, a significant improvement on the performance of link error prediction model can be obtained.

#### 4.4 Comparison of effective SINR mappings

In order to find out the simple and accurate L2S interface that should be used at the system level simulations the comparison of different ESM methods is necessary. The initial comparison of the effective SINR mapping begins from the comparison of the information measure functions. The information measure functions for linear ESM, EESM and MI-ESM are plotted in Figure 4.4 in order to show their characteristics. In the Figure 4.4 the exponential and mutual information functions are shifted using proper  $\beta$  scaling parameter in order to illustrate the similarities in shape between mutual information and exponential function.

These information measure functions have two different shape characteristics: convexity and sigmoid (so called S-shape). The information measure of linear ESM is a convex function, but EESM and MI-ESM information measure curves are sigmoidal. This difference partially occurs due to the modulation format being involved in EESM and MI-ESM, and it has a significant impact on how various SINR samples are relatively weighted in a certain information measure function [27]. Since the amount of information that a channel can pass with a certain modulation scheme should follow sigmoidal curves [27], and EESM and MI-ESM have sigmoidal shape, they describe the information transferred by individual SINR samples better.

Linear information measure weights all SINR samples equally, and the resulting effective SINR describes the performance for a given channel "on

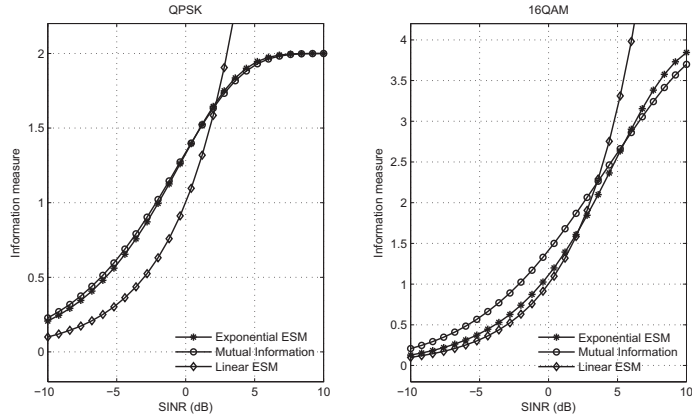


**Figure 4.4.** The information measure functions for Linear ESM, EESM and MI-ESM for QPSK, 16QAM modulation. Here, SINR value is divided by  $\beta$  adjustment parameter for proper shifting.

average”. Taken into account the used modulation, this quality measure is then used to predict the link performance. Instead, EESM information measure puts higher weight on lower SINR samples and less weight on higher SINR samples. Thus, the critical in terms of final error probability SINR samples dominate the resulting effective SINR value.

MI-ESM in general behaves similarly as EESM, but the weight of lowest and highest SINR samples are limited by lower and upper limits of the information measure function. Such evaluation of SINR samples allows crucial SINR samples to dominate on performance quality estimation. Comparison of EESM and MI-ESM in terms of channel capacity given in [27] shows that mutual information measure function better characterizes the system performance. However, the EESM function with accurate adjustment of  $\beta$  scaling factor is able to reach high accuracy as shown in Publication I and confirmed later in [20, 102]. Hence, in general the EESM model can be considered as a specific approximation of the MI-ESM model [20]. Both, EESM and MI-ESM are recommended for multi-carrier system performance evaluation in [27]. The cumulative distribution function (CDF) of resulting effective SINR values calculated by means of linear, exponential and mutual information measure functions are illustrated in Figure 4.5.

Understanding the behavior of relative weighting for convex and sigmoidal functions an improvement for the convex information measure is proposed in Publication I. Due to boundedness of sigmoid the bounding of convex linear information measure can be done so that crucial SINR sam-

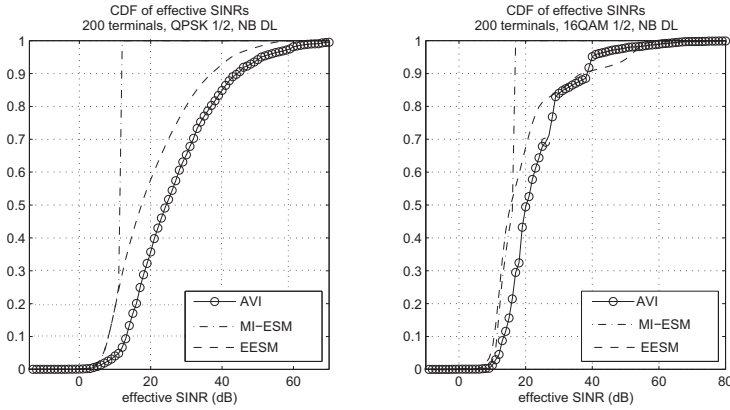


**Figure 4.5.** The CDF of effective SINR values calculated using linear, exponential and mutual ESM models.

ples will have more contribution on final quality measure. Since EESM and MI-ESM information measures are bounded by the modulation format and the bandwidth, these characteristics should define the thresholds for linear information measure to indicate crucial SINRs. In linear ESM approach the modulation scheme and the bandwidth are involved in performance estimating through coded BLER calculations. So, the bounds for linear information measure may be derived from the link level look-up tables. Based on the information measure bounded from above and below an improved linear ESM method is proposed in Publication I.

These three link error prediction models can be compared in terms of BLERs as shown in Publication I in order to capture their differences. As shown in [14] the BLER performance curves produced by the link level simulations are steep due to involved turbo coding. Therefore, the relatively small difference in effective SINR values can lead to relatively high difference in BLER values. Thus, the comparison in terms of BLERs brings more insight into the accuracy estimation of the link prediction modeling. The simulation results presented in Publication I show sufficiently similar block error rate probabilities obtained through EESM and MI-ESM models. Detailed comparison as well as simulation results may be found in Publication I.

The ESM methods can be distinguished by its flexibility for the link adaptation design as shown in [20, 98]. The MI-ESM model is considered

to be the most suitable for radio resource management, since it differentiates between the modulation and coding scheme explicitly. Moreover, MI-ESM allows that different MCS schemes are applied for different sub-carriers. Other ESM methods do not have this flexibility. Only one MCS scheme appropriate for the transmission can be applied inside the coded block. Moreover, a unique scaling parameter is adjusted for combination of modulation and coding rate in case of linear and exponential ESM models. The separation of modulation and coding models for EESM model is proposed in [102]. The effective SINRs are converted to bit-SINRs dividing them by modulation scaling parameters obtained from the link level simulations. The average of bit-SINRs adjusted by coding scaling parameter is mapped to BLER looking up AWGN performance curves. The separation of modulation and coding models is attractive for hybrid-ARQ as well as power and rate adaptation for mixed modulation cases.

Finally, the different ESM models can be compared in terms of simulation time since the prediction of the link quality is the most time consuming operation on the system level. The calculation of effective SINR using EESM and MI-ESM mapping is much more time demanding than simple averaging. Therefore, the speed-up of effective SINR calculations on the system level is desired. The simplification of effective SINR calculation using EESM mapping is proposed in Publication VI. The proposed model reduces the number of quality measures involved into compression without any considerable loss in the system spectral efficiency. The results illustrated in Publication VI show that significant CPU time savings can be achieved. The simplification model presented in Publication VI can be applied to general ESM mapping (4.18).

#### 4.5 EESM distribution

The knowledge of statistical distribution of effective SINR is crucial for performance analysis. It can be utilized to estimate accurately the block error probability. It can be used for system performance evaluation through the capacity. Moreover, it can be applied at the system level simulations in order to reduce the simulation time.

The asymptotic distribution of EESM is analytically established and verified by simulations in Publication III. The exponential effective SINR is the L2S interface model recommended by 3GPP community for 3GPP

LTE network. The asymptotic distribution of effective SINR is established through the following steps. First, the moment generating function of post-processed SINR is derived. Then the cumulant generating function of effective SINR is obtained in the case of independent and  $m$ -dependent quality measures. Finally, the mean and the variance of the effective SINR for normal approximation are derived. The normal approximation is justified using the properties of moments and cumulants. The detailed description and derivations of the analyses as well as simulation results may be found in Publication III.

The impact of adaptive modulation and HARQ on the distribution of effective SINR is analytically established and validated by simulations in Publication IV. In order to take into account link adaptation, the distribution of effective SINR is proposed to be modeled as mixture of normal distributions with specified mean and variances. Including HARQ process in the analysis the effective SINR after several retransmission can be modeled as normal random variable due to the independence of retransmissions. The details of the analyses as well as simulation results may be found in Publication IV.

The correlation properties of the sub-carrier post-processed SINR values are taken into account in the effective SINR distribution analyzes in Publication V. The asymptotic distribution of the effective SINR is analytically derived using moment generating function of post-processed SINR to be normal. Moreover, the distribution of the effective SINR obtained from the compression of small number of quality measures is accurately approximated by the convolution of two Gamma distributions with derived parameters. The details of the analyses as well as simulation results may be found in Publication V.

## 4.6 Discussion

In this chapter the evolution of L2S interface methodology is reviewed starting from traditional approach applicable for single carrier system and extending to the effective SINR mapping proposed for multi-carrier system. The most promising approaches for link error prediction model are considered to be MI-ESM and EESM mapping. The reason is the sigmoidal property of informational measure function, since sigmoidal curve does not underestimate low SINR values nor does it overestimate high

SINR values. Moreover, sigmoidal curve gives the best fitting for the practical channel codes with a certain modulation scheme as claimed in [27]. The EESM and MI-ESM approaches has been compared in terms of effective SINRs, information measure functions and resulting BLERs in order to capture the differences in Publication I. Table 4.1 summarizes the comparison results. In spite of the fact that in general the EESM model can be considered as an approximation of the MI-ESM model, it also describes the receiver performance for the system level with very high accuracy.

The EESM mapping is standardized as a link quality prediction model for LTE performance evaluation. At the system level simulations the measurement of the link quality is the most time consuming operation [24]. In order to reduce the simulation time the speed up of exponential effective SINR calculation is developed in Publication VI. The proposed speed up is independent of employed information measure function and is applicable for general ESM mapping.

In order to involve precisely L2S interface model into the system capacity evaluation the distribution of exponential effective SINR is established analytically and verified by simulations. Starting from independent and  $m$ -dependent cases the asymptotic distribution of effective SINR is derived in Publication III. Taking into account the impact of adaptive modulation and coding as well as Hybrid-ARQ the asymptotic distribution of effective SINR is established in Publication IV. The distribution of the effective SINR based on correlated post-processed SINR values is derived in Publication V. The way how the established distributions of effective SINR can be utilized in the system capacity metric is presented in Chapter 5. The derived analytical results provide an efficient way to evaluate system level performance with a confidence in a computational efficient but realistic manner. Moreover, it allows to evaluate the impact of mobility, link adaptation as well as retransmissions on the system performance as shown in Chapter 5.

**Table 4.1.** Comparison of the effective SINR mapping methods.

<b>Properties</b>	<b>Linear ESM</b>	<b>EESM</b>	<b>MI-ESM</b>
Information Measure	linear	exponential	mutual information
Shape of IM	convex	sigmoid	sigmoid
Modulation and coding	joint	joint possible to separate	separate
Resulting BER	not equivalent to EESM or MI-ESM	equivalent to MI-ESM	equivalent to EESM
Computational efficiency	fast and simple	demanding possible to speed up	demanding



## 5. System capacity and performance evaluation

The 3GPP LTE and future 4G wireless systems aim at providing high peak data rates of up to 100 Mbps for high mobility and up to 1 Gbps for low mobility [49, 73, 84] using MIMO–OFDM transmission. In this chapter we discuss the capacity of MIMO–OFDM system, summarize the approaches for dynamic rank adaptation and evaluate the performance results of MIMO–OFDM transmission.

### 5.1 MIMO capacity

The significant increase in the capacity using multiple antennas firstly demonstrated in [107], [76], [33, 96] predicted the linear growth of capacity gain proportional to  $\min(N_t, N_r)$  relative to SISO system in the rich scattering environment. Since then MIMO systems has been widely studied in order to characterize the theoretical and practical issues how to approach promised capacity limits.

In this chapter we focus on MIMO channel capacity in information theoretic sense, that is defined as maximum mutual information between the channel input and output for single user time invariant channel. Ergodic channel capacity used here for time varying channel is defined as the maximum mutual information averaged over all channel states.

Let's consider some central concepts for flat fading MIMO signal model defined as

$$\underset{N_r \times 1}{\mathbf{y}} = \underset{N_r \times N_t}{\mathbf{H}} \underset{N_t \times 1}{\mathbf{s}} + \underset{N_r \times 1}{\mathbf{n}}, \quad (5.1)$$

where  $\mathbf{y}$  is the received signal vector,  $\mathbf{s}$  is the transmitted signal vector with covariance  $E(\mathbf{s}\mathbf{s}^H) = \mathbf{Q}$ ,  $\mathbf{n}$  contains the measurement noise with covariance  $N_0$ ,  $\mathbf{H}$  is the channel response and is assumed as i.i.d. zero mean and unit variance complex Gaussian channel for the central con-

cepts discussed here. The channel model has a crucial effect on the capacity. Recent reviews of capacity issues for the wider range of channel models including for example spatial correlated fading, multipath delay spread, cluster angle spread can be found, e.g., in [21, 35, 39]. The influence of correlated noise to the capacity can be found in [31, 86].

The capacity differs depending on the level of knowledge of CSI at the transmitter. If CSI is available at the receiver only and there is no CSI available at the transmitter, the ergodic capacity is maximized for equal power allocation among all transmit antennas as follows [33, 96, 97]

$$\begin{aligned} C &= \max_{\text{Tr}(\mathbf{Q}) \leq P} E_{\mathbf{H}} \left( \log_2 \det \left( \mathbf{I}_{N_r} + \frac{1}{N_0} \mathbf{H}^H \mathbf{Q} \mathbf{H} \right) \right) \\ &= E_{\mathbf{H}} \left( \log_2 \det \left( \mathbf{I}_{N_r} + \frac{P}{N_0 N_t} \mathbf{H}^H \mathbf{H} \right) \right) \text{ b/s/Hz}. \end{aligned} \quad (5.2)$$

Ergodic capacity in (5.2) scales linearly with  $\min(N_t, N_r)$  in all SNRs [33, 96, 97], since the channel rank is at most  $\min(N_t, N_r)$ , meaning that channel has at most  $\min(N_t, N_r)$  eigenmodes. Thus, the capacity can be interpreted as a sum of capacities of each of these eigenmodes.

If CSI is available not only at the receiver but also at the transmitter the capacity over  $\mathbf{Q}$  subject to power constraint can be optimized by a waterfilling as follows [96, 97]

$$\begin{aligned} P_i &= \left( \mu - \frac{N_0}{\lambda_i} \right)_+, \\ C &= \sum_{i=1}^{\min(N_t, N_r)} E \left( \log_2 \left( 1 + \frac{P_i}{N_0} \lambda_i \right) \right) \text{ b/s/Hz}, \end{aligned} \quad (5.3)$$

where  $\mu$  is defined by the total power constraint  $\sum_{i=1}^{\min(N_t, N_r)} P_i = P$ , function  $\square_+$  sets negative numbers to zero,  $\lambda_i$  are nonzero eigenvalues of  $\mathbf{H}^H \mathbf{H}$ .

The impact of feedback information at the transmitter can be analyzed via comparison of waterfilling capacity (5.3) with equal power capacity (5.2). As shown in [21, 35] the gains provided by waterfilling solution are significant at low SNR and negligible at high SNR. With transmitter CSI transmit array gain can be achieved, but its importance is diminished at high SNR. Spatial multiplexing gain and diversity gain can be obtained without transmitter CSI by using SFBC/STTD and PARC schemes as discussed in Chapter 2.

Note, that presented theoretical capacity results are challenging to achieve in practice due to implicit assumptions on infinite block size, existing of capacity-reaching code, optimum decoding, transceiver imperfection, uncertainty in noise and interference.

### 5.1.1 MIMO–OFDM capacity

The ergodic capacity as a measure of goodness of fading channel can be extended to the OFDM-based spatial multiplexing system given in equation (2.1). For the MIMO–OFDM system (2.1) with  $K$  sub-carriers the ergodic capacity with equal power allocation is defined as [8, 16]

$$C = E_{\mathbf{H}} \left( \frac{1}{K} \sum_{k=1}^K \log_2 \det \left( \mathbf{I}_{N_s} + \frac{P}{N_s} \mathbf{W}_k^H \mathbf{H}_k^H \mathbf{R}_k^{-1} \mathbf{H}_k \mathbf{W}_k \right) \right) \text{ b/s/Hz}. \quad (5.4)$$

The ergodic capacity (5.4) can be expressed in terms of the post-processing SINR as [32]

$$C = E_{\gamma} \left( \frac{1}{K} \sum_{k=1}^K \sum_{n=1}^{N_s} \log_2 (1 + \gamma_{n,k}) \right) \text{ b/s/Hz}, \quad (5.5)$$

where  $\gamma_{n,k}$  is the post-processed SINR of the  $n$ -th spatial data stream on the  $k$ -th sub-carrier.

The capacity (5.5) for MIMO–OFDM performance evaluation is analyzed in Publication III and alternative representation of the capacity by means of the effective SINR (4.34),  $\gamma_n^{\text{eff}}$ , is established as

$$C \approx \sum_{n=1}^{N_s} \log_2 \left( 1 + E_{\gamma}(\gamma_n^{\text{eff}}) \right). \quad (5.6)$$

The capacity expression (5.6) is more practical for the the system level performance evaluation, since on the system level the quality of the link is estimated through the effective SINR, not post-processed SINR. The capacity (5.6) includes directly system level quality measure (effective SINR) and indirectly link level quality measure (post-processed SINR,  $\beta_n$  scaling parameter, that are used to map to the effective SINR). Other system level capacity evaluations presented in [63] and used for 3GPP LTE performance evaluation in [46] involve additional tuning coefficients and do not take into account L2S interface model, that is heavily used in the system level.

Knowing the distribution of the effective SINR the analytic form of the capacity (5.6) is defined with the confidence in the mean value as shown in Publication III. Such analytic representation of the capacity allows to evaluate the impact of the mobility Publication III as well as adaptive modulation and HARQ Publication IV on the MIMO–OFDM system performance and reflects precisely mapping method between the system level and the link level.

## 5.2 Rank adaptation using capacity approach

The radio resource management is developed to provide MIMO-aware algorithms covering link adaptation, rank adaptation, Hybrid-ARQ and packet scheduling [58].

The goal of rank adaptation algorithm is to optimize the selection of MIMO transmission scheme for each scheduled user, since the standard of 3GPP LTE includes several transmission schemes, e.g., presented in section 2.3.5.

Due to varying MIMO channel experienced by the user the base station can adapt the number of spatial multiplexing streams of MIMO transmission to the changing conditions dynamically. The rank adaptation is the procedure of selecting the rank of the MIMO transmission, meaning selecting the transmission scheme, at the base station based on the measurements and feedback information as discussed in section 3.3.2

The straightforward approach for the rank adaptation is to select the optimum MIMO rank at the terminal side by maximizing the total instantaneous user throughput [103]. In Publication II the capacity-based rank adaptation is proposed, where instantaneous capacity is evaluated over the whole bandwidth as

$$C = \sum_{k=1}^K \log_2 \det \left( \mathbf{I}_{N_t} + \frac{P}{N_t} \mathbf{H}_k^H \mathbf{R}_k^{-1} \mathbf{H}_k \right) \text{ b/s/Hz}, \quad (5.7)$$

and precoding is not taken into account.

The proposed rank adaptation algorithm exhibits similar performance as the throughput-based rank adaptation given in [103]. However, proposed scheme is beneficial in terms of lower complexity, it takes into account channel conditions and provides speed up in the CPU time.

## 5.3 Results on performance

The computer simulations provide several benefits such as performance evaluation of future communication systems that can be controlled and repeated as discussed in Chapter 3. The perfect performance evaluation can not be done by computer simulations due to high complexity of modeling. However, the obtained simulation results in predefined scenarios can be used for comparison in order to find the potential limits of the performance [23].

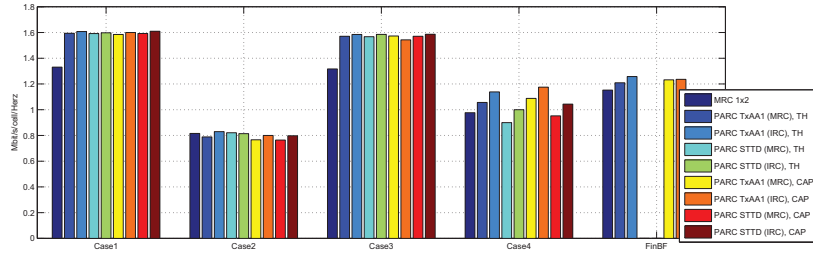


**Figure 5.1.** 3GPP LTE DL spectral efficiency for Infinite and Finite Buffer in 3GPP Cases 1-4, PARC is used for a dual stream transmission, TxAA1 [103] (CDD-like open-loop MIMO MIMO rank 1 scheme discussed in section 2.3.5) or STTD is used for a single stream transmission with MRC or IRC receiver. Two different rank adaptation procedures are used in the simulations: capacity-based rank adaptation denoted by CAP and total instantaneous user throughput rank adaptation [103] denoted by TH.

As discussed in section 3.5 there is no unique and preferred measure of performance for wireless communication systems. But the most essential measures of performance from the system operator point of view are system capacity and spectral efficiency. From the user point of view an average user throughput and cell-edge user throughput are important measures.

In Publication II the spectral efficiency and user throughput performance results in 3GPP LTE downlink predefined macro deployment scenarios are compared in order to analyze the effect of environment and mobility to multi-stream transmission and gathered MIMO multiplexing gains. Figure 5.1 illustrates the spectral efficiency results obtained in 3GPP Cases 1-4 predefined scenarios. The simulation results show that MIMO transmission in all low mobility 3GPP LTE macro cell scenarios provide 10-20% gain in spectral efficiency with infinite buffer traffic model. More realistic finite buffer traffic load reduces spatial multiplexing benefits. MIMO multiplexing gains demonstrated in high mobility environments are clearly lower.

In Publication III the impact of mobility on the system performance is analyzed through the comparison of ergodic capacity results in LTE DL network under realistic mobility scenarios. Figure 5.2 illustrates the impact of mobility on ergodic system capacity (5.6) in low (3kmph), medium (30 kmph) and high (120kmph) mobility scenarios. The results show a clear loss of average spectral efficiency in high mobility scenarios due to 70% drop in the mean value of effective SINR. This is caused by chosen robust MCS as well as outdated channel feedback.

In Publication IV the effect of adaptive modulation combined with HARQ is analyzed through the comparison of ergodic capacity results in LTE DL network under realistic mobility scenarios. Figure 5.3 illustrates the impact of link adaptation and retransmission to the ergodic system capacity (5.6) in low (3kmph), medium (30 kmph) and high (120kmph) mobility scenarios. The results show that by using adaptive modulation combined with HARQ the performance loss caused by mobility is significantly smaller. Moreover, the performance gap to non-adaptive and non-robust case grows as mobility speed grows.

The aforementioned fully dynamic system level simulation results with explicitly modeled user mobility give a realistic view of mobile MIMO-OFDM system performance.

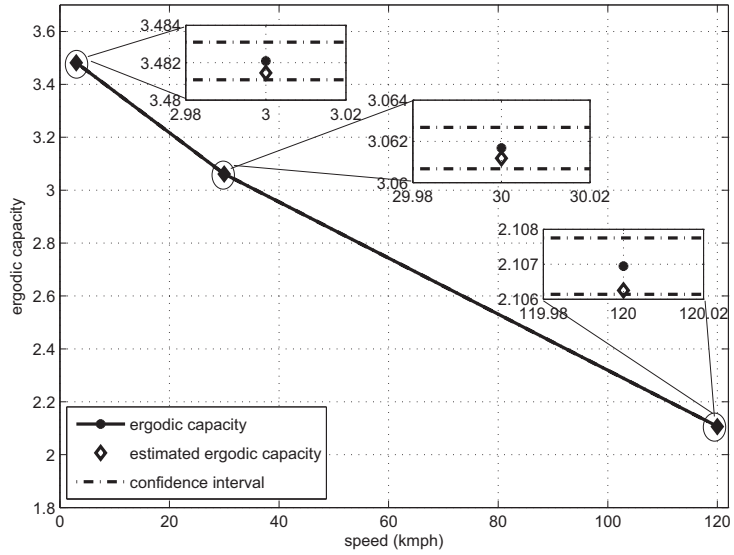


**Figure 5.2.** Ergodic system capacity (5.6) with a confident in the mean value of the effective SINR in different mobility scenarios (3kmph, 30kmph and 120 kmph).

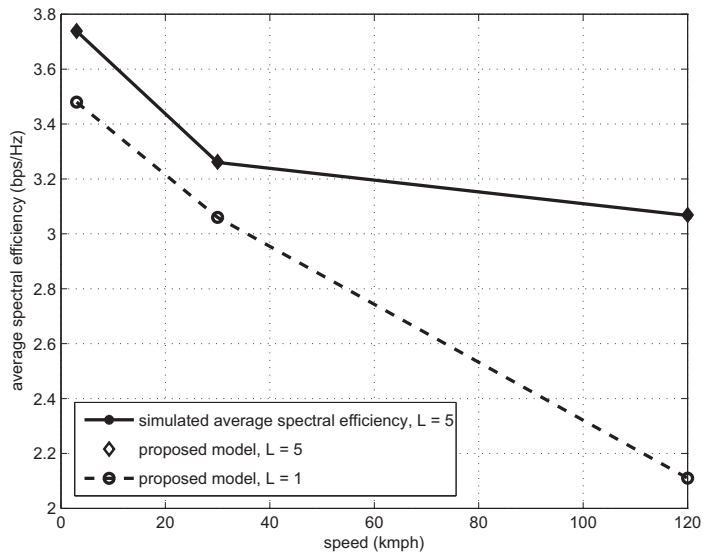


**Figure 5.3.** Ergodic system capacity (5.6) for single MCS level and for multiple MCS levels with HARQ in different mobility scenarios (3kmph, 30kmph and 120 kmph).





## 6. Summary

Multi-stream multi-carrier wireless transmission techniques are expected to provide high data rates and spectral efficiency required by forthcoming 3GPP Long Term Evolution standards (3GPP LTE and 3GPP LTE-A) [1]. In order to evaluate the performance of LTE under realistic mobility scenarios, design of many layer 1, layer 2 and radio resource management functions as well as link-to-system interface are crucial. This thesis focuses on optimization of the link-to-system interface and on developing efficient system capacity measures at the system level for performance evaluation of beyond 3G wireless communication network in realistic multi-cell mobility scenarios.

First, the traditional L2S interface approaches are studied and compared to the effective SINR mapping methods. The comparison demonstrated the high accuracy of the effective SINR mapping methods such as EESM and MI-ESM in terms of error rate and user throughput.

In this thesis a computationally efficient method for calculation of the effective SINR mapping at the system level is developed. The accuracy of the proposed fast approximation for effective SINR is evaluated both analytically by establishing error bounds and in simulations in a typical 3GPP LTE downlink scenarios. The results show that proposed solution reduces significantly CPU time of system level simulations with no loss in the accuracy of the results.

The L2S interface at the system level has been studied further and the distribution of the effective SINR using moment generation function of post-processed SINRs is derived. The established distribution allows to utilize the system capacity measure with the confidence and to analyze the impact of link adaptation and HARQ on the system performance.

In this thesis an overview of the capacity for MIMO-OFDM system is provided and the ergodic capacity based on the effective SINR is ana-

lyzed. The ergodic MIMO–OFDM system capacity is evaluated analytically through the mean value of the effective SINR. The impact of user mobility to the system performance via mobility factor is established by using mapping between classical Shannon capacity and the proposed MIMO–OFDM system capacity. The obtained analytical results have been validated by simulations in realistic multi-cell scenarios using 3GPP LTE downlink network model.

In case of adaptive modulation and coding, a mixture distribution model is used to evaluate an overall system performance. The statistical properties of the effective SINR including the correlation is analyzed even more thoroughly. The asymptotic distribution of the effective SINR is analytically derived using the moment generating function of post-processed sub-carrier SINRs. An approximation of the effective SINR mapped from a small number of post-processed sub-carrier SINRs is proposed and analytically derived. The established distributions of the effective SINR can be utilized through the mean value in the system capacity measure.

Designing new radio resource management functions are necessary to support and to exploit the benefits of multi-stream transmission in the wireless network. One of them is the dynamic rank adaptation supported at the receiver side. It should allow fast and efficient adaptation to the varying channel conditions in the presence of intercell interference. In this thesis the dynamic rank adaptation based on the system level capacity is proposed in order to provide an efficient and computationally simple measure of number of spatial layers.

The research work made by the author not only solves optimization problems in the L2S interface but also leads to the new research topics and open problems. Possible topics of future research include more accurate estimation of the distribution for the effective SINR since the established asymptotic distribution is not practical for the small packet transmission scenarios. Also, of interest is the optimization of L2S interface for the MI-ESM mapping method, that is much more complex to analyze using analytical tools. Due to the development of the 3GPP standards the potential future research topics include the extension of the derived techniques for multi-user MIMO–OFDM transmission in 3GPP LTE network. In addition, the system level performance studies can be extended by including different scheduling strategies to the simulation methodology since they influence significantly the final system performance.

# Bibliography

- [1] 3GPP. <http://www.3gpp.org>.
- [2] 3GPP RAN. <http://www.3gpp.org/RAN>.
- [3] 3GPP. Physical Layer Aspects for Evolved UTRA. Technical Report TR 25.814 TSG RAN Rel. 7, 3G Partnership Project, September 2006. <http://www.3gpp.org/ftp/>.
- [4] 3GPP. Requirements for Evolved UTRA and Evolved UTRAN. Technical Report TR 25.913 TSG RAN Rel. 6, 3G Partnership Project, March 2006. <http://www.3gpp.org/ftp/>.
- [5] 3GPP. Evolved Universal Terrestrial Radio Access (E-UTRA); Physical channels and modulation. Technical Report TS 36.211 TSG RAN, 3G Partnership Project, September 2007. Rel. 8.
- [6] 3GPP2. 1xEV-DV Evaluation Methodology. Technical Report 3GPP2/TSG-C.R1002 V13, 3GPP2, September 2003. [www.3gpp2.org/Public\\_html/specs/](http://www.3gpp2.org/Public_html/specs/).
- [7] 3GPP2. cdma2000 Evaluation Methodology. Technical Report C.R1002-B V1.0, 3GPP2, December 2009. [http://www.3gpp2.org/Public\\_html/specs](http://www.3gpp2.org/Public_html/specs).
- [8] M. Ahmed, A. Alexiou, F. Kharrat, M. Lamarca, R. Pintenet, F. Rey, J. Sala, and D. Samardzija. MTMR Baseband Transceivers Need for Intra-system and Inter-system (UMTS/WLAN) Reconfigurability. Technical Report IST-2000-30116 D3.3.1, Information Society Technologies FITNESS Project, August 2003. <http://www.telecom.ntua.gr/fitness/>.
- [9] S. M. Alamouti. A Simple Transmit Diversity Technique for Wireless Communications. *IEEE Journal on Selected Areas in Communications*, 16(8):1451–1458, October 1998.
- [10] A. Alexiou, T. Al-Gizawi, D. Axiotis, D. Bourse, S. Buljore, A. Chatzikonstantinou, L. EliceGUI, J. Gosteau, R. Karimi, J. Kruys, F. Lazarakis, K. Pappas, R. Pintenet, and S. Simoens. System-Level Simulation Methodology Defined. Technical Report IST-2000-30116 D4.1, Information Society Technologies FITNESS Project, August 2002. <http://www.telecom.ntua.gr/fitness/>.

- [11] A. Alexiou, D. Astély, K. Brüninghaus, P. Coronel, M. Döttling, M. Fuchs, J. Giese, M. Haardt, M. Hennhöfer, T. Jiang, É. Jorswieck, A. Kapur, Z. Li, A. Medles, T. Mousley, M. Olsson, K. Roberts, S. Rouquette-Léveil, W. Schott, A. Sezgin, P. Skillermark, V. Stankovic, P. Svedman, S. Visuri, D. Wang, T. Wild, and E. Zimmermann. Assessment of Advanced Beamforming and MIMO Technologies. Technical Report IST-2003-507581 issue 1.0, D2.7, WINNER, February 2005. <http://www.ist-winner.org/DeliverableDocuments/>.
- [12] M. Anas, F. Calabrese, P.-E. Östling, K. Pedersen, and P. Mogensen. Performance Analysis of Handover Measurements and Layer 3 Filtering for UTRAN LTE. In *Proceedings of the 18th IEEE International Symposium on Personal, Indoor and Mobile Radio Communications, PIMRC 2007*, pages 1–5, September 2007.
- [13] K. Baum, T. Kostas, P. Sartori, and B. Classon. Performance Characteristics of Cellular Systems with Different Link Adaptation Strategies. *IEEE Transactions on Vehicular Technology*, 52:1497–1507, November 2003.
- [14] Y. Blankenship, P. Sartori, B. Classon, V. Desai, and K. Baum. Link Error Prediction Methods for Multicarrier Systems. In *Proceedings of the 60th IEEE Vehicular Technology Conference, VTC2004-Fall*, volume 6, pages 4175–4179, September 2004.
- [15] V.M. Bogachev and I.G. Kiselev. Optimum Combining of Signals in Space – Diversity Reception. *Telecommunications and Radio Engineering*, 34/35:83–85, October 1980.
- [16] H. Bölcskei, D. Gesbert, and A. Paulraj. On the Capacity of OFDM–Based Spatial Multiplexing Systems. *IEEE Transactions on Communications*, 50(2):225–234, February 2002.
- [17] K. Brüninghaus, D. Astély, T. Salzer, S. Visuri, A. Alexiou, S. Karger, and G. Seraji. Link Performance Models for System Level Simulations of Broadband Radio Access Systems. In *Proceedings of the 16th IEEE International Symposium on Personal, Indoor and Mobile Radio Communications, PIMRC 2005*, volume 4, pages 2306–2311, September 2005.
- [18] G. Caire, G. Taricco, and E. Biglieri. Capacity of bit-interleaved Channels. *Electronics Letters*, 32(12):1060, June 1996.
- [19] F. Cavalcanti and S. Andersson. *Optimizing Wireless Communication Systems*. Springer Science, New York USA, 1st edition, 2009. 514 p.
- [20] X. Chen, L. Wan, Z. Gao, Z. Fei, and J. Kuang. The Application of EESM and MI-based Link Quality Models for Rate Compatible LDPC Codes. In *Proceedings of the 66th IEEE Vehicular Technology Conference, VTC2007-Fall*, pages 1288–1292, September 2007.
- [21] C.-N. Chuah, D. Tse, J. Kahn, and R. Valenzuela. Capacity Scaling in MIMO Wireless Systems Under Correlated Fading. *IEEE Transactions on Information Theory*, 48(3):637–650, August 2002.
- [22] L. Correia. *Mobile Broadband Multimedia Networks: Techniques, Models and Tools for 4G*. Elsevier, Oxford, CA USA, 1st edition, 2006. 600 p.

- [23] E. Dahlman, S. Parkvall, J. Sköld, and P. Beming. *3G Evolution: HSPA and LTE for Mobile Broadband*. Elsevier, Oxford, CA USA, 2nd edition, 2008. 648 p.
- [24] K. Doppler. *In-band Relays for Next Generation Communication Systems*. Aalto University School of Science and Technology, Doctoral thesis, 2010. <http://lib.tkk.fi/Diss/2010/isbn9789526031255/>.
- [25] M. Döttling. Assessment of Advanced Beamforming and MIMO Technologies. Technical Report IST-2003-507581 WINNER D2.7 v. 1.1, IST-WINNER, February 2005. [http://projects.celtic-initiative.org/winner+/  
/](http://projects.celtic-initiative.org/winner+/).
- [26] Ericsson. Considerations on the System Performance Evaluation of HS-DPA using OFDM Modulation. Technical Report TSG-RAN WG1 Meeting 34 R1-030999, 3GPP, October 2003. <http://www.3gpp.org/ftp/>.
- [27] Ericsson. Effective SIR Mapping for Modelling Frame Error Rates in Multiple-state Channels. Technical Report 3GPP2-C30-20030429-010, 3GPP2, April 2003. <ftp://ftp.3gpp2.org/>.
- [28] Ericsson. System Level Evaluation of OFDM – further considerations. Technical Report TSG-RAN WG1 Meeting 35 R1-031303, 3GPP, November 2003. <http://www.3gpp.org/ftp/>.
- [29] Ericsson. System Level Evaluation of OFDM – initial evaluation. Technical Report TSG-RAN WG1 Meeting 35 R1-031304, 3GPP, November 2003. <http://www.3gpp.org/ftp/>.
- [30] Ericsson. Summary of Downlink Performance Evaluation. Technical Report TSG-RAN WG1 Meeting 49 R1-072578, 3GPP, May 2007. <http://www.3gpp.org/ftp/>.
- [31] F. Farrokhi, G. Foschini, A. Lozano, and R. Valenzuela. Link-Optimal BLAST Processing With Multiple-Access Interference. In *Proceedings of the 52nd IEEE Vehicular Technology Conference, VTC2000-Fall*, volume 1, pages 87–91, September 2000.
- [32] G. Foschini, D. Chizhik, C. Papadias, and R. Valenzuela. Analysis and Performance of Some Basic Space–Time Architectures. *IEEE Journal on Selected Areas in Communications*, 21(3):303–320, April 2003.
- [33] G. J. Foschini and M. J. Gans. On Limits of Wireless Communications in a Fading Environments When Using Multiple Antennas. *Wireless Personal Communications*, 6(3):311–335, January 1998.
- [34] F. Frederiksen and T. Kolding. Performance and modeling of WCDMA/HSDPA transmission/H-ARQ schemes. In *Proceedings of the 56th IEEE Vehicular Technology Conference, VTC2002-Fall*, volume 1, pages 472–476, September 2002.
- [35] D. Gasbert, M. Shafi, D. Shiu, P. Smith, and A. Naguib. From Theory To Practice: An Overview of MIMO Space-Time Coded Wireless Systems. *IEEE Journal on Selected Areas in Communications*, 21(3):281–302, April 2003.

- [36] D. Gesbert, M. Shafi, D.-S. Shiu, P. Smith, and A. Naguib. From Theory to Practice: An Overview of MIMO Space-Time Coded Wireless Systems. *IEEE Journal on Selected Areas in Communications*, 21(3):281–302, April 2003.
- [37] A. Ghosh, W. Xiao, R. Ratasuk, A. Rottinghaus, and B. Classon. Multi-Antenna System Design for 3GPP LTE. In *Proceedings of IEEE International Symposium on the Wireless Communication Systems, ISWCS 2008*, pages 478–482, October 2008.
- [38] A. Goldsmith. *Wireless Communications*. Cambridge University Press, 1rd edition, 2005. 644 p.
- [39] A. Goldsmith, S. Jafar, N. Jindal, and S. Vishwanath. Capacity Limits of MIMO Channels. *IEEE Journal on Selected Areas in Communications*, 21(5):684–702, June 2003.
- [40] S. Grant, C. Jung-Fu, L. Krasny, K. Molnar, and Y.-P. Wang. Per-Antenna-Rate-Control (PARC) in Frequency Selective Fading with SIC-GRABKE Receiver. In *Proceedings of the 60th IEEE Vehicular Technology Conference, VTC2004-Fall*, volume 2, pages 1458–1462, September 2004.
- [41] M. Gudmundson. Correlation Model for Shadow Fading in Mobile Radio Systems. *Electronics Letters*, 27(23):2145–2146, November 1991.
- [42] S. Hämmäläinen, H. Holma, and K. Sipilä. Advanced WCDMA Radio Network Simulator. In *Proceedings of the 10th IEEE International Symposium on Personal, Indoor and Mobile Radio Communications, PIMRC 1999*, pages 509–604, September 1999.
- [43] S. Hämmäläinen, P. Slanina, M. Hartman, A. Lappeteläinen, H. Holma, and O. Salonaho. A Novel Interface Between Link and System Level Simulations. In *Proceedings of the ACTS Mobile Telecommunications Summit*, pages 599–604, October 1997.
- [44] M. Hata. Empirical Formula for Propagation Loss in Land Mobile Radio Services. *IEEE Transactions on Vehicular Technology*, VT-29(3):317–325, August 1980.
- [45] X. He, K. Niu, Z. He, and J. Lin. Link Layer Abstraction in MIMO-OFDM System. In *Proceedings of IEEE International Workshop on the Cross Layer Design, IWCLD 2007*, pages 41–44, September 2007.
- [46] H. Holma and A. Toskala. *LTE for UMTS – OFDMA and SC-FDMA Based Radio Access*. John Wiley & Sons, Ltd, 1st edition, 2009. 464 p.
- [47] A. Hottinen, O. Tirkkonen, and R. Wichman. *Multi-antenna Transceiver Techniques for 3G and Beyond*. A John Wiley and Sons, Ltd, 1rd edition, 2003. 342 p.
- [48] A. Huebner, E. Schuehlein, M. Bossert, E. Costa, and H. Haas. A Simple Space-Frequency Coding Scheme with Cyclic Delay Diversity for OFDM. In *Proceedings of the 5th European Personal Mobile Communications Conference*, pages 106–109, April 2000.

- [49] ITU-R. Requirements, evaluation criteria and submission templates for the development of IMT-Advanced. Technical Report M.[IMT.REST], International Telecommunication Union, October 2008. <http://www.itu.int/md/R07-SG05-C-0068/en>.
- [50] W. Jakes. *Microwave Mobile Communications*. John Wiley and Sons Inc, New York, 1st edition, 1974.
- [51] M. Jeruchim, P. Balaban, and K. Shanmugan. *Simulation of Communication Systems: Modeling, Methodology and Techniques*. Springer, Kluwer Academic/Plenium Publishers, New York USA, 2nd edition, 2000. 924 p.
- [52] P. Kela, J. Puttonen, N. Kolehmainen, T. Ristaniemi, T. Henttonen, and M. Moisio. Dynamic Packet Scheduling Performance in UTRAN Long Term Evolution Downlink. In *Proceedings of the 3rd IEEE International Symposium on Wireless Pervasive Computing, ISWPC 2008*, pages 308–313, May 2008.
- [53] J. Ketchum, B. Bjerke, I. Medvedev, S. Nanda, and R. Walton. PHY abstraction based on PER prediction. Technical Report 802.11-04/0269r0, IEEE, March 2004. <http://www.ieee802.org/11/>.
- [54] S. M. Key. *Fundamentals of Statistical Signal processing: Estimation Theory*. Prentice Hall International, Inc, 1rd edition, 1993. 625 p.
- [55] J. Khoja, M. Al-Shalash, and V. Prabhu. Dynamic System Simulator for the Modeling of CDMA Systems. In *Proceedings of the International Mobility and Wireless Access Workshop, MobiWac 2002*, pages 50–58, October 2002.
- [56] K. J. Kim and J. Yue. Joint Channel Estimation and Data Detection Algorithms for MIMO–OFDM Systems. In *Proceedings of the 36th Asilomar Conference on Signals, Systems and Computers*, volume 2, pages 1857–1861, November 2002.
- [57] N. Kolehmainen, J. Puttonen, P. Kela, T. Ristaniemi, T. Henttonen, and M. Moisio. Channel Quality Indication Reporting Schemes for UTRAN Long Term Evolution Downlink. In *Proceedings of the 67th IEEE Vehicular Technology Conference, VTC2008-Spring*, pages 2522–2526, May 2008.
- [58] I. Kovàcs, M. Kuusela, E. Virtej, and K. Pedersen. Performance of MIMO Aware RRM in Downlink OFDMA. In *Proceedings of the 67th IEEE Vehicular Technology Conference, VTC2008-Spring*, pages 1171–1175, May 2008.
- [59] J. Kurjenniemi, T. Henttonen, and J. Kaikkonen. Suitability of RSRQ Measurement for Quality Based Inter-Frequency Handover in LTE. In *Proceedings of the IEEE International Symposium on Wireless Communication Systems, ISWCS 2008*, pages 703–707, October 2008.
- [60] M. Lampe, T. Giebel, H. Rohling, and W. Zirwas. PER Prediction for PHY Mode Selection in OFDM Communication Systems. In *Proceedings of the IEEE Global Communications Conference, CLOBECOM 2003*, volume 1, pages 25–29, December 2003.



- [61] E. Malkamäki, F. de Ryck, and C. Mouro. A Method for Combining Radio Link Simulations and System Simulations for a Slow Frequency Hopped Cellular System. In *Proceedings of the 44th IEEE Vehicular Technology Conference, VTC1994-Spring*, pages 1145–1149, June 1994.
- [62] E. Malkamäki, F. de Ryck, and C. Mouro. A Novel Approach to Processing Speed Enhancement for Dynamic CDMA Network Simulations. In *Proceedings of the 60th IEEE Vehicular Technology Conference, VTC2004-Fall*, volume 6, pages 4301–4305, September 2004.
- [63] P. Mogensen, N. Wei, I. Kovács, F. Frederiksen, A. Pokhariyal, K. Pedersen, T. Kolding, K. Hugl, and M. Kuusela. LTE Capacity compared to the Shannon Bound. In *Proceedings of the 65th IEEE Vehicular Technology Conference, VTC2007-Spring*, pages 1234–1238, April 2007.
- [64] J. Monserrat, R. Fraile, N. Cardona, and J J. Gozalvez. Effect of Shadowing Correlation Modeling on the System Level Performance of Adaptive Radio Resource Management Techniques. In *Proceedings of the 2nd IEEE International Symposium on Wireless Communication Systems, ISWCS 2005*, pages 460–464, September 2005.
- [65] Technical Specification Group Radio Access Network. Feasibility Study for Orthogonal Frequency Division Multiplexing (OFDM) for UTRAN Enhancement. Technical Report TR 25.892 TSG RAN Rel. 5, 3GPP, June 2004. <http://ftp.3gpp.org/specs/>.
- [66] Nortel Networks. Effective SIR Computation for OFDM System Level Simulations. Technical Report TSG-RAN WG1 Meeting 35 R1-031370, 3GPP, November 2003. <http://www.3gpp.org/ftp/>.
- [67] Nortel Networks. OFDM EESM simulation Results for System-Level Performance Evaluations, and Text Proposal for Section A. 4.5 of TR 25.892. Technical Report TSG-RAN WG1/TSG-RAN WG4 Ad Hoc R1-040089, 3GPP, January 2004. <http://www.3gpp.org/ftp/>.
- [68] Nokia. Performance Evaluation – Uplink Summary. Technical Report TSG-RAN WG1 Meeting 49 R1-072261, 3GPP, May 2007. <http://www.3gpp.org/ftp/>.
- [69] Special Mobile Group of ETSI. Universal Mobile Telecommunications System (UMTS); Selection Procedures for the Choice of Radio Transmission Technologies of the UMTS. Technical Report TR 101 112 v3.2.0, European Telecommunications Standards Institut, April 1998. <http://www.etsi.org>.
- [70] Y. Okumura, E. Ohmori, T. Kawano, and K. Fukuda. Field Strength and Its Variability in VHF and UHF Land-Mobile Radio Service. *Review of the Electrical Communication Laboratory*, 16(1):825–873, September 1968.
- [71] H. Olofsson, M. Almgren, C. Johansson, M. Höök, and F. Kronestedt. Improved Interface Between Link Level and System Level Simulations Applied to GSM. In *Proceedings of the 6th IEEE International Conference on Universal Personal Communications, UCUPC 1997*, pages 79–83, October 1997.



- [72] Orange, China Mobile, KPN, NTT, DoCoMo, Sprint, T-Mobile, Vodafone, and Telecom Italia. LTE Physical Layer Framework for Performance Evaluation. Technical Report TSG RAN WG1 RL1 R1-070674, 3G Partnership Project, February 2007. <http://www.3gpp.org/ftp/>.
- [73] S. Parkvall and D. Astely. The Evolution of LTE towards IMT-Advanced. *Journal of Communications*, 4(3):146–154, April 2009.
- [74] C. Passerini and G. Falciasecca. Modeling of Orthogonality Factor Using Ray-Tracing Predictions. *IEEE Transactions on Wireless Communications*, 3(6):2051–2059, November 2004.
- [75] A. Paulraj, D. Gore, R. Nabar, and H. Bolcskei. An Overview of MIMO Communications – A Key to Gigabit Wireless. *Proceedings of the IEEE*, 92(2):198–218, February 2004.
- [76] A. Paulraj and T. Kailath. Increasing Capacity in Wireless Broadcast Systems Using Distributed Transmission/Directional Reception (DTDR). Technical Report 5,345,599, United States Patent, September 1994. <http://patft.uspto.gov/netacgi/>.
- [77] K. Pedersen, F. Frederiksen, T. Kolding, T. Lootsma, and P. Mogensen. Performance of High-Speed Downlink Packet Access in Coexistence With Dedicated Channels. *IEEE Transactions on Vehicular Technology*, 56(3):1262–1270, May 2007.
- [78] K. Pedersen, T. Kolding, I. Kovács, G. Monghal, F. Frederiksen, and P. Mogensen. Performance Analysis of Simple Channel Feedback Schemes for a Practical OFDMA System. *IEEE Transactions on Vehicular Technology*, 58(9):5309–5314, November 2009.
- [79] K. Pedersen and P. Mogensen. The Downlink Orthogonality Factors Influence on WCDMA System Performance. In *Proceedings of the 56th IEEE Vehicular Technology Conference, VTC2002-Fall*, volume 4, pages 2061–2065, September 2002.
- [80] A. Pokhariyal, K. Pedersen, G. Monghal, I. Kovács, C. Rosa, T. Kolding, and P. Mogensen. HARQ Aware Frequency Domain Packet Scheduler with Different Degrees of Fairness for the UTRAN Long Term Evolution. In *Proceedings of the 65th IEEE Vehicular Technology Conference, VTC2007-Spring*, pages 2761–2765, May 2007.
- [81] Qualcomm. Applicability of ECM Approach for System Simulations. Technical Report TSG RAN WG1 Meeting 33 R1-03-1014, 3GPP, October 2003. <http://ftp.3gpp.org/specs/>.
- [82] R. Ratasuk, A. Ghosh, and B. Classon. Quasi-static Methodology to Predict Link-Level Performance. In *Proceedings of the 55th IEEE Vehicular Technology Conference, VTC2002-Spring*, pages 1298–1302, May 2002.
- [83] C. Ribeiro, K. Hugl, M. Lampinen, and M. Kuusela. Performance of Linear Multi-User MIMO Precoding in LTE System. In *Proceedings of the 3rd IEEE International Symposium on Wireless Pervasive Computing, ISWPC 2008*, pages 410–414, May 2008.

- [84] M. Roberts, M. Temple, R. Mills, and R. Raines. Evolution of the Air Interface of Cellular Communications Systems toward 4G Realization. *IEEE Communications Surveys and Tutorials*, 8(1):2–23, March 2007.
- [85] H. Sampath, S. Talwar, J. Tellado, V. Erceg, and A. Paulraj. A Fourth-Generation MIMO-OFDM Broadband Wireless System: Design, Performance, and Field Trial Results. *IEEE Communication Magazine*, 40(9):141–149, September 2002.
- [86] A. Scaglione, P. Stoica, S. Barbarossa, G. Giannakis, and H. Sampath. Optimal Designs For Space-Time Linear Precoders and Decoders. *IEEE Transactions on Signal Processing*, 50(5):1051–1064, August 2002.
- [87] A. Seeger, M. Sikora, and A. Klein. Variable Orthogonality Factor: a Simple Interface between Link and System Level Simulation for High Speed Downlink Packet Access. In *Proceedings of the 58th IEEE Vehicular Technology Conference, VTC2003-Fall*, volume 4, pages 2531–2534, September 2003.
- [88] S. Sessia, I. Toufik, and M. Baker. *LTE, The UMTS Long Term Evolution: From Theory to Practice*. A John Wiley and Sons, Ltd, 1rd edition, 2009. 648 p.
- [89] S. Shakkottai and T. Rappaport. Research Challenges in Wireless Networks: A Technical Overview. In *International Symposium of Wireless Personal Multimedia Communications*, pages 12–18, October 2002.
- [90] R. Srinivasan, J. Zhuang, L. Jalloul, R. Novak, and J. Park. IEEE 802.16m Evaluation Methodology Document. Technical Report IEEE 802.16m-08/004r4, IEEE 802.16, November 2008. <http://www.ieee802.org/16/>.
- [91] G. Stüber, J. Barry, S. McLaughlin, Y. Li, M. Ingram, and T. Pratt. Broadband MIMO-OFDM Wireless Communications. *Proceedings of the IEEE*, 92(2):271–294, February 2004.
- [92] V. Tarokh, N. Seshadri, and A. Calderbank. Space-Time Block Codes from Orthogonal Design. *IEEE Transactions on Information Theory*, 45(5):1456–1467, July 1995.
- [93] Lucent Technologies. Link Error Prediction for E-DCH. Technical Report TSG RAN WG1 Meeting 33 R1-030777, 3GPP, August 2003. <http://www.3gpp.org/ftp/>.
- [94] Lucent Technologies. Reverse Link Hybrid ARQ: Link Error Prediction Methodology Based on Convex Metric. Technical Report TSG-C WG3 20030401-020, 3GPP2, April 2003. <ftp://ftp.3gpp2.org/>.
- [95] A. Tee, S. Yoon, and J. Cleveland. Link-to-System Interface Simulation Methodologies. Technical Report C802.20-04/67, IEEE 802.20 Working Group on Mobile Broadband Wireless Access, June 2004. <http://www.ieee802.org/20/>.
- [96] I. E. Telatar. Capacity of Multi-Antenna Gaussian Channels. *European Transactions on Telecommunications*, 10(6):585–595, December 1999.
- [97] D. Tse and P. Vismanath. *Fundamentals of Wireless Communication*. University Press, Cambridge UK, 1st edition, 2005. 586 p.

- [98] E. Tuomaala and H. Wang. Effective SINR Approach of Link to System Mapping in OFDM/Multi-carrier Mobile Network. In *Proceedings of the 2nd IEEE International Conference on Mobile Technology, Applications and Systems*, pages 1–5, April 2005.
- [99] M. K. Varanasi and T. Guess. Optimum Decision Feedback Multi-User Equalization with Successive Decoding Achieves the Total Capacity of the Gaussian Multiple-Access Channel. In *Proceedings of the 31st Asilomar Conference on Signals, Systems and Computers*, volume 2, pages 1405–1409, November 1997.
- [100] E. Virtež, M. Kuusela, and E. Tuomaala. System Performance of Single-User MIMO in LTE Downlink. In *Proceedings of the 19th IEEE International Symposium on Personal, Indoor and Mobile Radio Communications, PIMRC 2008*, pages 1–5, September 2008.
- [101] A. Wacker, J. Laiho-Steffens, K. Sipilä, and M. Jäsberg. Static Simulator for Studying WCDMA Radio Network Planning Issues. In *Proceedings of the 49th IEEE Vehicular Technology Conference, VTC1999-Spring*, pages 2436–2440, May 1999.
- [102] L. Wan, S. Tsai, and M. Almgren. A Fading-Intensive Performance Metric for a Unified Link Quality Model. In *Proceedings of the IEEE Wireless Communications and Networking Conference, WCNC2006*, pages 2110–2114, September 2006.
- [103] N. Wei, A. Pokhariyal, T. Sørensen, T. Kolding, and P. Mogensen. Performance of MIMO with Frequency Domain Packet Scheduling in UTRAN LTE Downlink. In *Proceedings of the 65th IEEE Vehicular Technology Conference, VTC2007-Spring*, pages 1177–1181, September 2007.
- [104] J. Wigard and P. Mogensen. A Simple Mapping from C/I to FER and BER for a GSM Type of Air Interface. In *Proceedings of the 7th IEEE International Symposium on Personal, Indoor and Mobile Radio Communications, PIMRC 1996*, pages 78–82, September 1996.
- [105] J. Wigard, T. Nielsen, H. Michaelsen, and P. Mogensen. BER and FER Prediction of Control and Traffic Channels for a GSM Type of Air Interface. In *Proceedings of the 48th IEEE Vehicular Technology Conference, VTC1998-Spring*, pages 1588–1592, May 1998.
- [106] J. Winters. Optimum Combining in Digital Mobile Radio with Co-Channel Interference. *IEEE Journal on Selected Areas in Communications*, 2:528–539, July 1984.
- [107] J. Winters. On the Capacity of Radio Communication Systems with Diversity in a Rayleigh Fading environment. *IEEE Journal on Selected Areas in Communications*, 5(5):871–878, June 1987.
- [108] L. Zheng and D. Tse. Diversity and Multiplexing: A Fundamental Trade-off in Multiple-Antenna Channels. *IEEE Transactions on Information Theory*, 49(5):1073–1096, May 2003.



# Original Publications





ISBN 978-952-60-4753-9  
ISBN 978-952-60-4754-6 (pdf)  
ISSN-L 1799-4934  
ISSN 1799-4934  
ISSN 1799-4942 (pdf)

**Aalto University**  
School of Electrical Engineering  
Department of Signal Processing and Acoustics  
[www.aalto.fi](http://www.aalto.fi)

**BUSINESS +  
ECONOMY**

**ART +  
DESIGN +  
ARCHITECTURE**

**SCIENCE +  
TECHNOLOGY**

**CROSSOVER**

**DOCTORAL  
DISSERTATIONS**